East Asian Monsoon and its Interannual Variability

KOICA Expert Program

for

Climate Prediction in Asia-Pacific

2007

Monsoon Interannual Variability

- Variability of monsoon
  - Indian summer monsoon
  - Western North Pacific summer monsoon
- Monsoon-ENSO interactions
- Simulation of monsoon variability
- Monsoon predictability- research at APCC
  - EA summer monsoon
  - EA winter monsoon
- Other topics

Variability of summer monsoon

Variability of summer monsoon

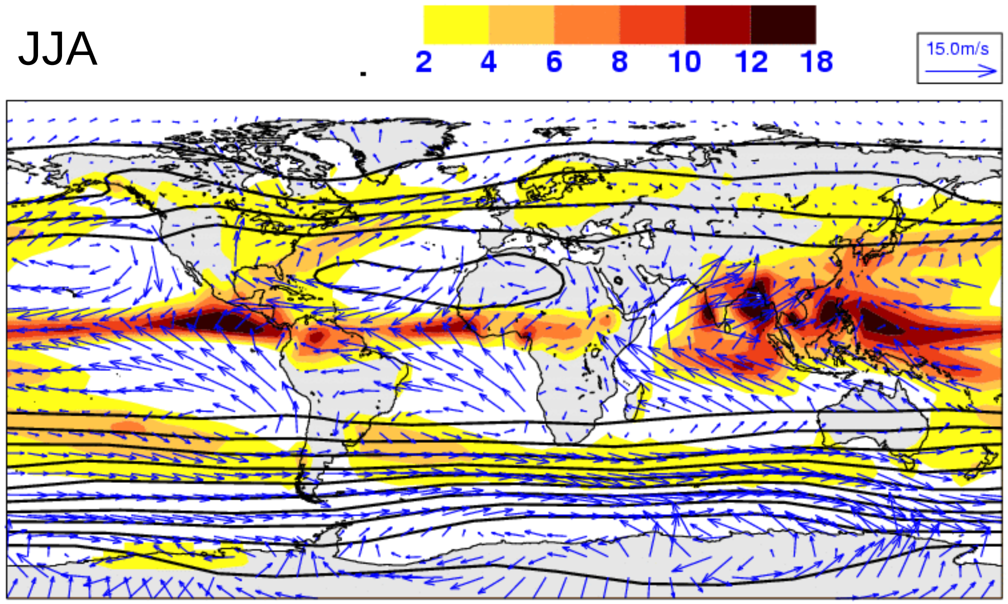

Precipitation and 1000mb wind- JJA

- Climatological mean of JJA circulation
- Q: how does it vary from year to year?

Variability of summer monsoon

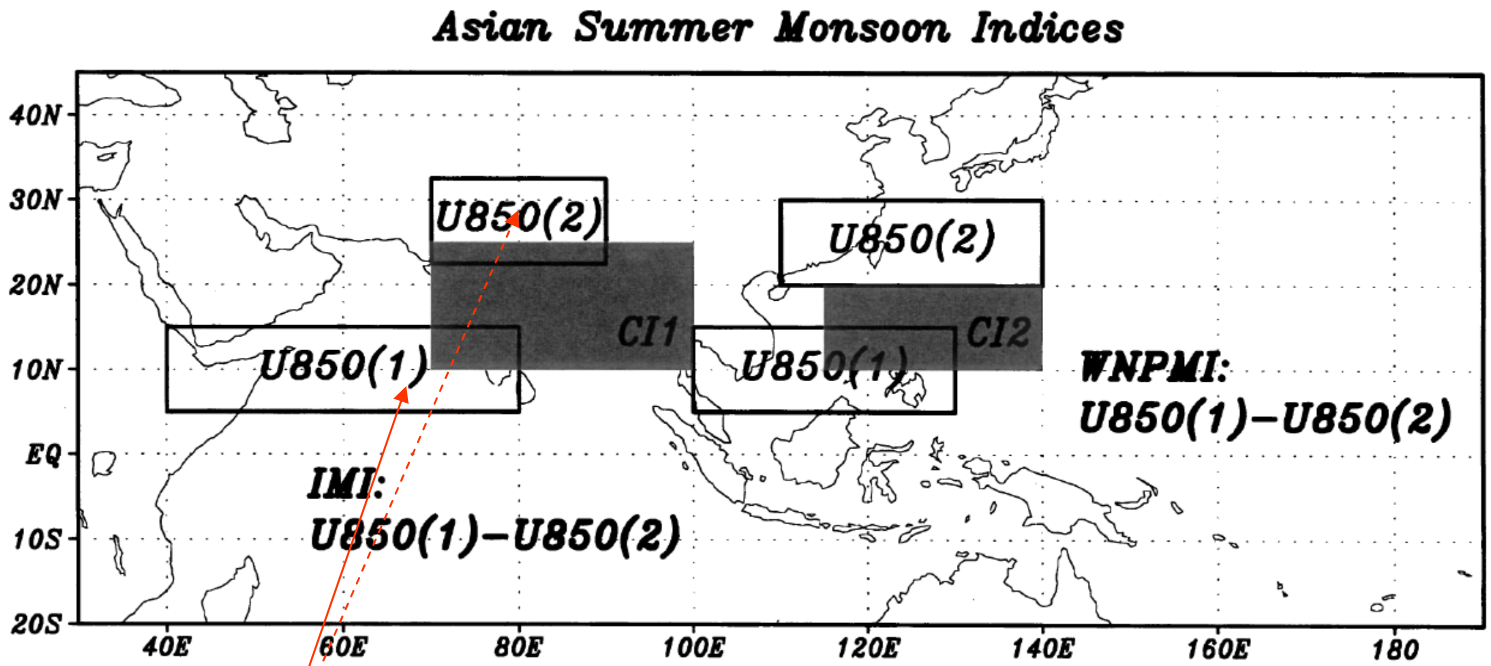

FIG. 2. Schematic diagram for the definition of the monsoon circulation indices, IMI and WNPMI. Shaded boxes indicate the regions for the rainfall indices, CI1 and CI2. The solid boxes denote regions where the zonal winds are used to define the monsoon circulation indices (refer to the text for details).

(from Wang and Fan 1999)

Basically measure vorticity/shear of mean flow

- Need simple measure (indices) to monitor monsoon variability
- IMI & WNPMI are used to monitor Indian and Western N Pac Monsoon
- How good are they?

Variability of summer monsoon

Results from Empirical Orthogonal Function (EOF) analysis

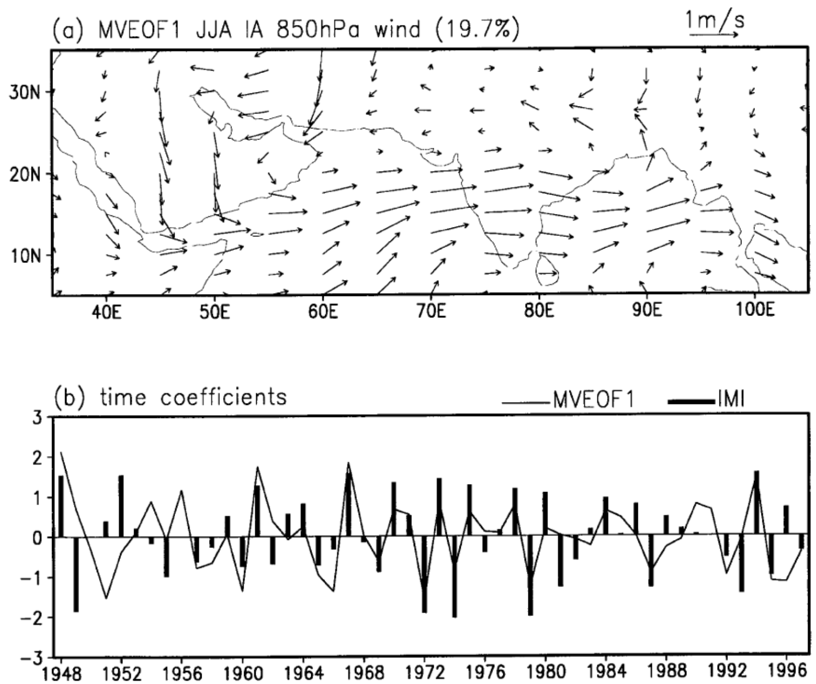

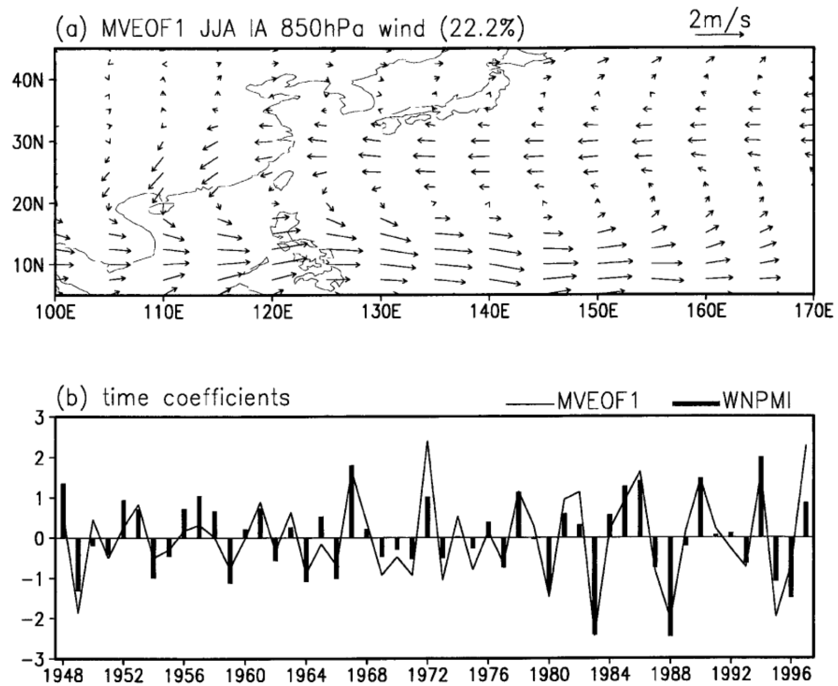

The leading multivariate EOF mode and (b) time coefficient of 850-hPa winds in the south Asian monsoon region for summer of 1948–97. The wind scales are displayed at the upper-right corners of (a) and (b). For comparison, the normalized IMI is plotted in (b) using bar charts.

Wang et al. (2001)

Variability of summer monsoon

- For a strong ISM:

(1) increases rainfall over India subcontinent

(2) enhanced Somali jet

- For a strong WNPSM:

(1) increased rainfall over the South China Sea and WNP

(2) a low-level elongated cyclonic circulation anomaly in the subtropical WNP

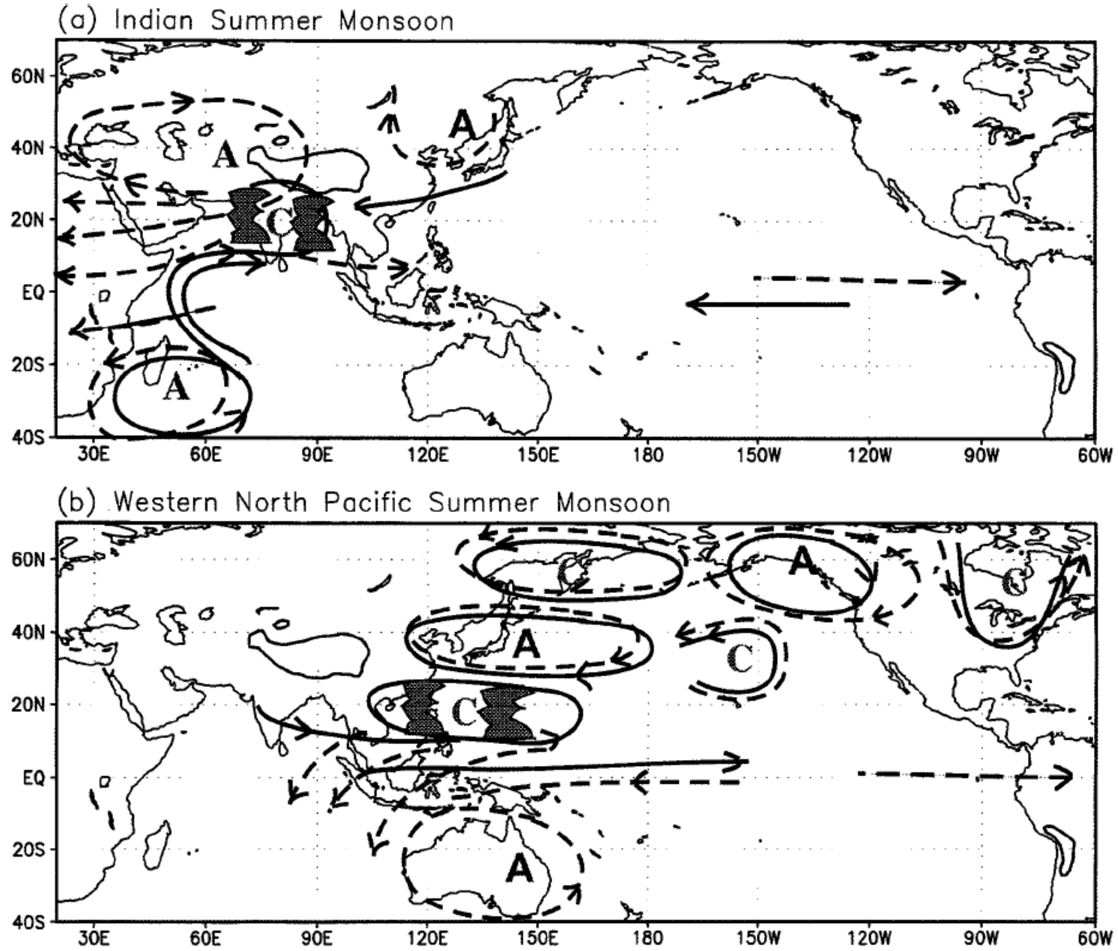

FIG. 12. Schematic diagrams showing the major circulation anomalies associated with (a) a strong Indian summer monsoon and (b) a strong western North Pacific summer monsoon. The lower-level and upper-level circulation anomalies are denoted by solid and dashed line, respectively. Letter "A" and "C" represent anticyclone and cyclone, respectively.

Wang et al. (2001)

Variability of summer monsoon

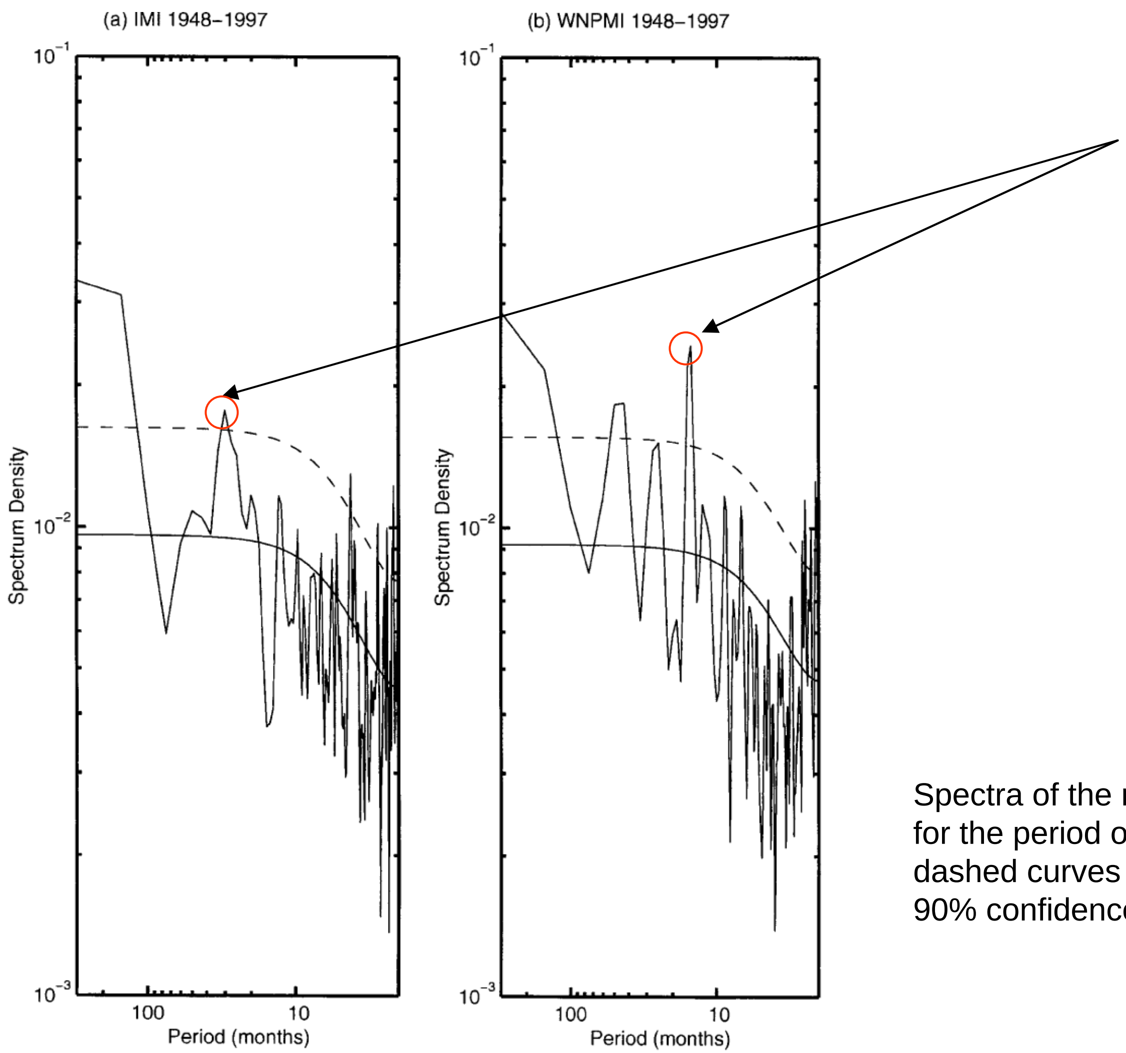

Spectra of the monthly mean (a) IMI and (b) WNPMI for the period of 1948–97. The smooth solid and dashed curves are for the red noise spectrum and its 90% confidence level.

Wang et al. (2001)

Variability of summer monsoon

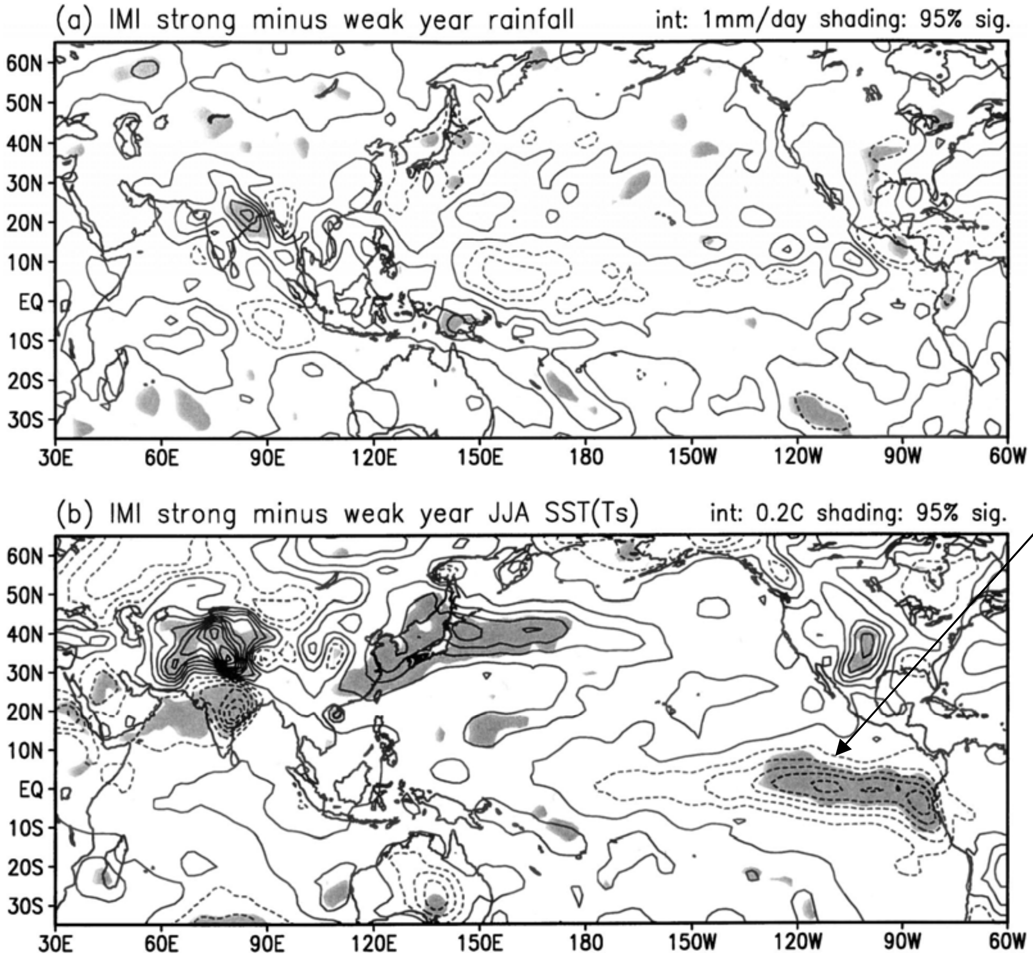

Notice the strong SST signal

Q: <u>what is the relationship between ISM and ENSO?</u>

Wang et al. (2001)

Composite difference of (a) summer rainfall and (b) sea (land) surface temperature between the strong and weak monsoon years with respect to the IMI. The contour interval is 1 mm day21 for the rainfall and 0.28C for SST. Shading denotes regions of difference at 95% confidence level. The rainfall data cover 1979–96 only.

Variability of summer monsoon

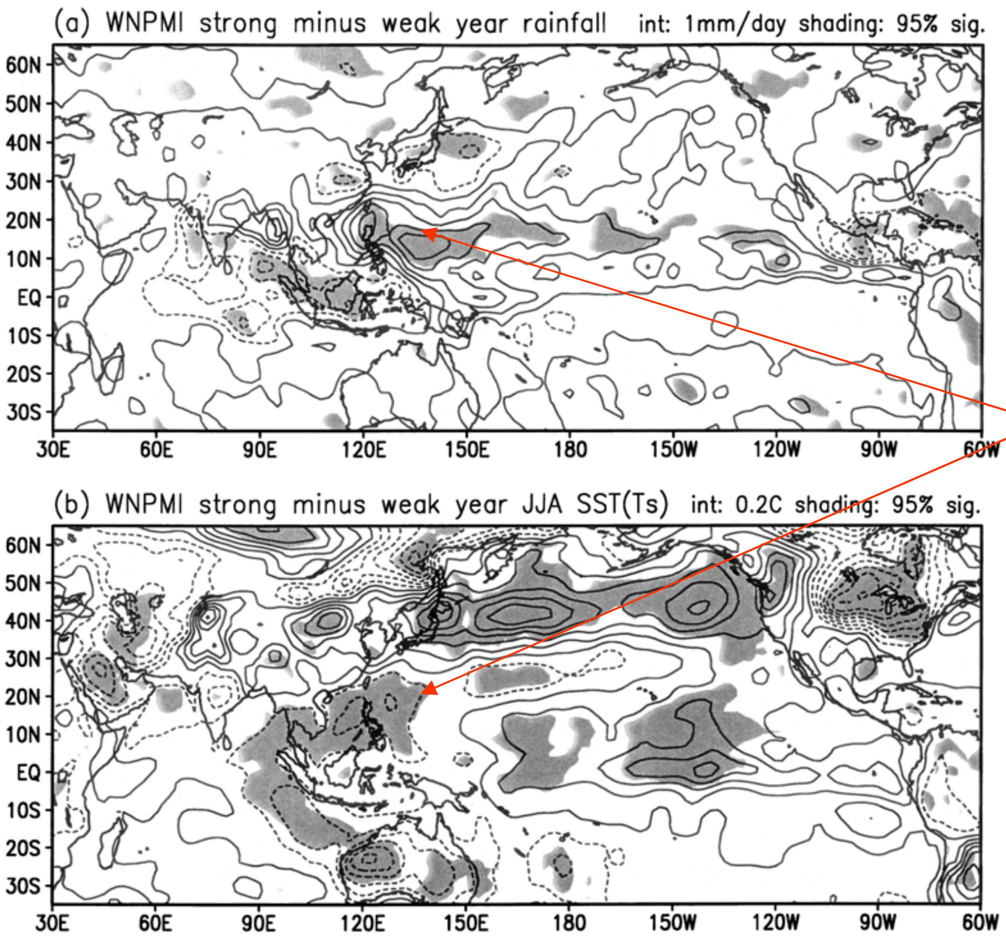

The salient feature is the **negative** SST-rainfall relationship. (<u>What does this imply?</u>)

GCMs forced by prescribed SST fail to capture this!

Same as previous figure, but for WNPSM

Wang et al. (2001)

Variability of summer monsoon (relationship w/ ENSO)

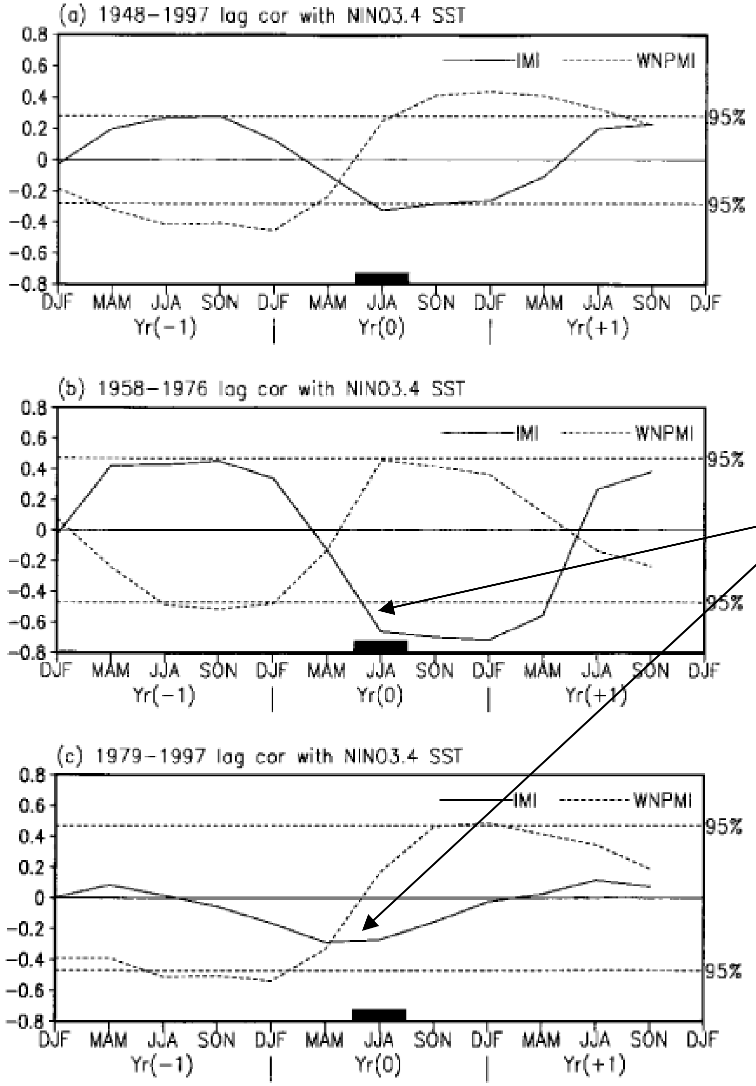

Decadal change of ISM-ENSO relationship

Lag correlation of the seasonal mean Nino-3.4 SST anomalies with reference to the IMI (solid) and WNPSMI (dashed) at the summer of year (0) for the period of (a) 1948–97, (b) 1958–76, and (c) 1979–97. The dashed horizontal lines indicate correlation of 95% confidence level.

Wang et al. (2001)

Monsoon-ENSO interaction

Monsoon-ENSO interaction (1)

Model simulation of monsoon response to ENSO

(AGCM forced by Tropical Pacific SST)

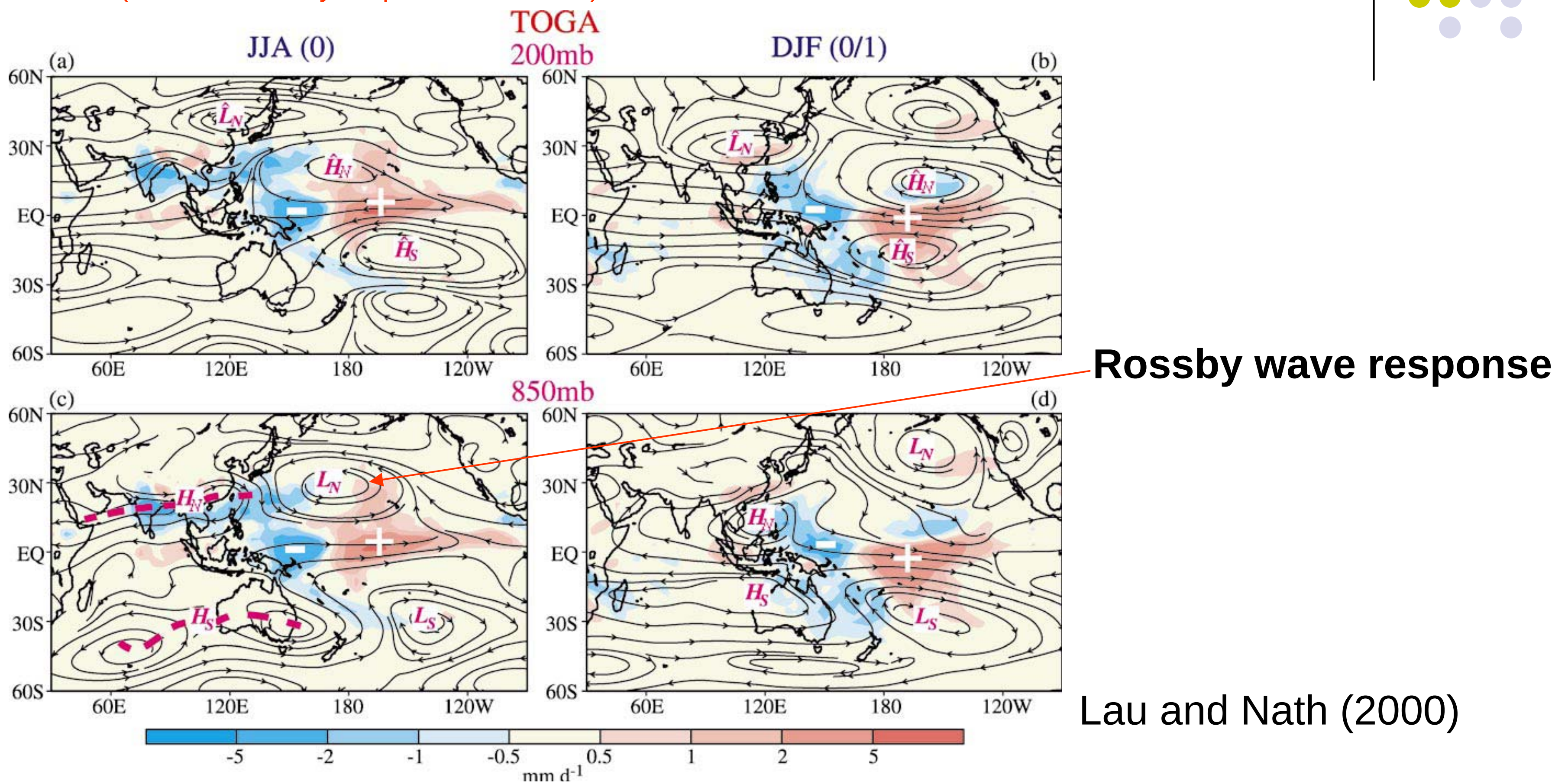

Lau and Nath (2000)

Distributions of the warm minus cold composite of the anomalous streamline patterns simulated in the TOGA experiment at [(a), (b)] 200 mb and [(c), (d)] 850 mb. Results are shown for the (left panels) JJA season of year (0) and (right panels) DJF season of year (0/1). The labels LN, LS, HN, and HS denote the 850-mb cyclonic and anticyclonic centers discussed in the text. The dashed lines in (c) depict the axes of the anomalous pressure ridges associated with HN and HS. The circulation centers at 200 mb are indicated using similar labels with the additional overcarat symbol. The composite precipitation anomalies for the corresponding seasons are presented using shading (see scale bar at bottom; units: mm day21). Centers of positive and negative precipitation anomalies along the equatorial Pacific are indicated by plus and minus signs, respectively.

Monsoon-ENSO interaction (1)

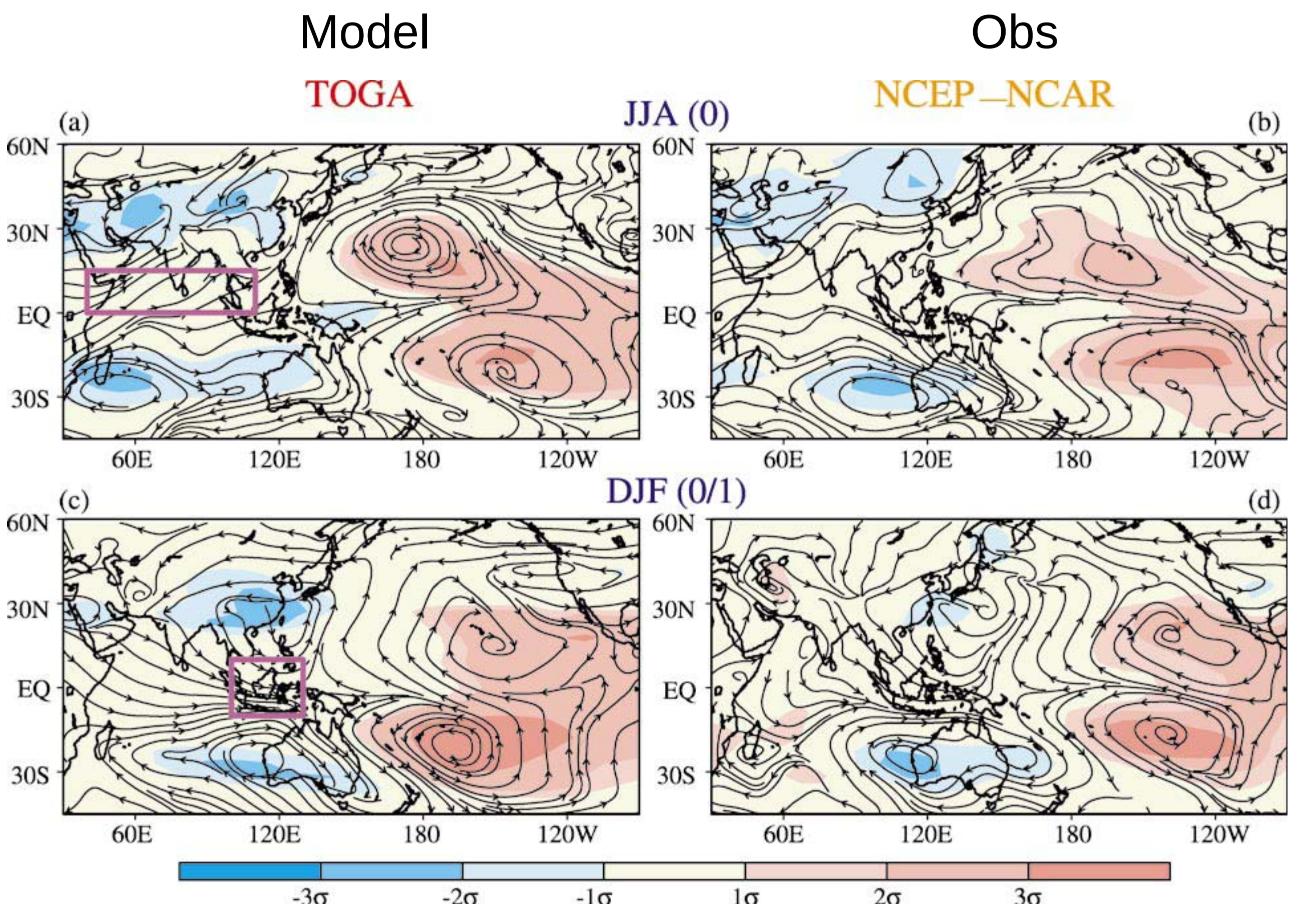

- Thickness and wind shear (200-850mb)
- Note the twin pairs of anticyclone/cyclone

Lau and Nath (2000)

As in previous figure, but for the streamline patterns obtained by subtracting the horizontal wind vector at 850 mb from the wind vector at 200 mb, and the thickness patterns obtained by subtracting the 850-mb height from the 200-mb height. Results are shown for the output from TOGA (left panels) and the NCEP–NCAR reanalysis data (right panels), and for the [(a), (b)] JJA season of year (0) and [(c), (d)] DJF season of year (0/1). The wind and height anomalies at individual pressure levels had been normalized by the local temporal standard deviation before differences were taken between the two levels. The purple rectangles in the left panels indicate the regions over which areal averages of zonal wind anomalies are to be computed for the construction of circulation indices.

Monsoon-ENSO interaction (2)-

effects on atmosphere-ocean variation over the Indian-western Pacific region

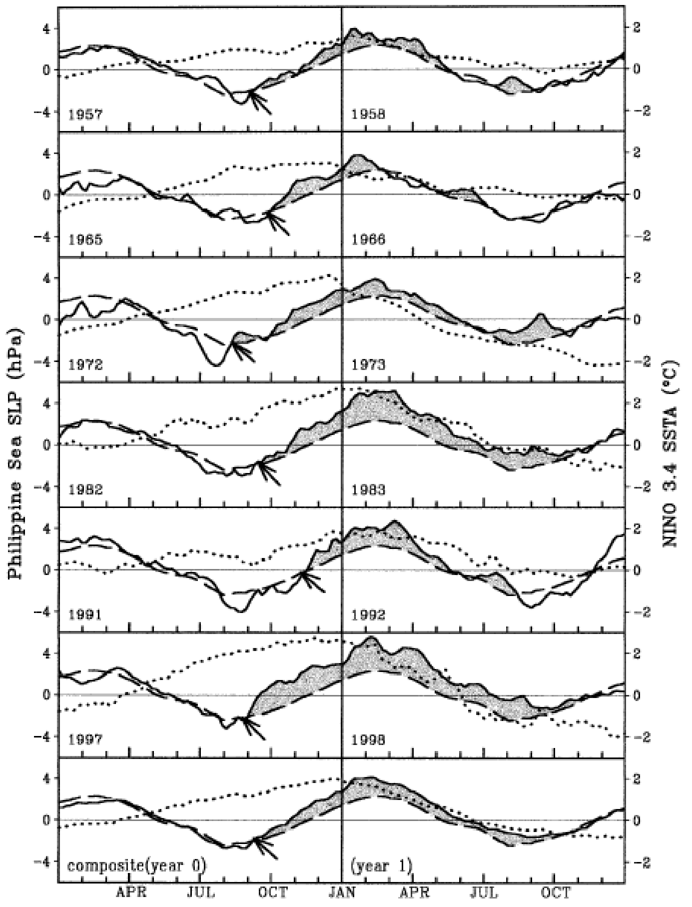

- For some ENSO events, air-sea interaction over WPAC is strong influenced
- (modeling studies require an interaction ocean)

The 7-pentad running mean (solid) and the climatological annual cycle (excluding the annual mean; long dashed) sea level pressure averaged over the Philippine Sea (108–208N, 1208–1508E) for six major El Nin˜o episodes and their composite with reference to the calendar month. The dotted curves are the corresponding 3-month running mean Nin˜o-3.4 SST anomalies. The arrows indicate the time that the anomalous PSAC occurs. The shading highlights the period during which the PSAC persists.

Formation of the Philippines Sea anticyclone

Wang and Zhang (2002)

Monsoon-ENSO interaction(2)

Sfc wind, vorticity and rainfall evolution during late summer/fall of yr(0)

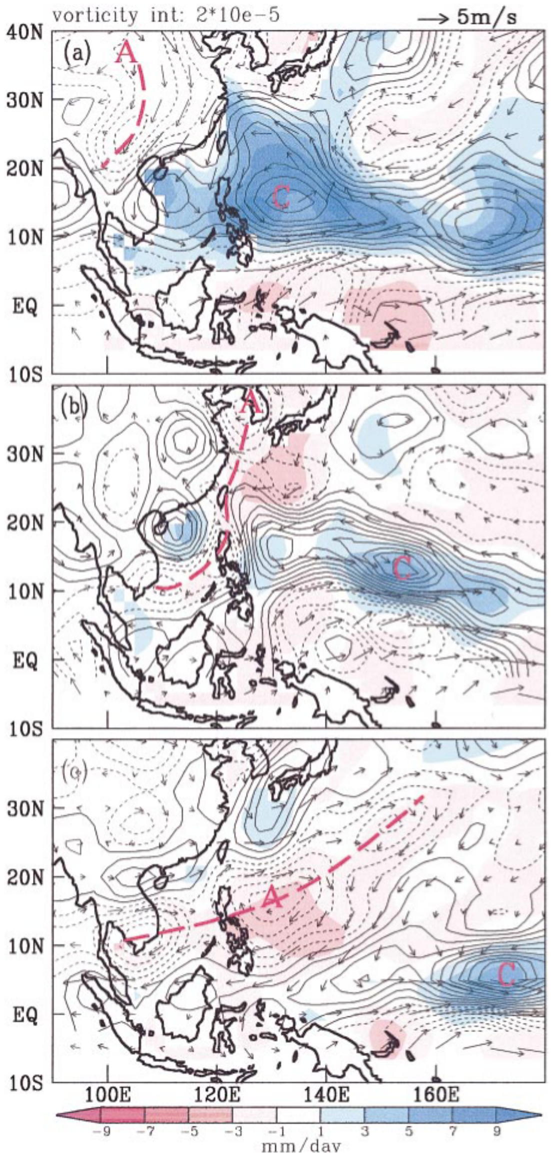

Composite pentad mean surface wind (arrows) and vorticity anomalies as well as precipitation rate anomalies (color shading in units of mm day21) during the (a) low pressure, (b) transition, and (c) high pressure phases of the intraseasonal oscillation associated with the PSAC formation. Letters‘‘A’’ and ‘‘C’’ mark the centers of the anomalous anticyclone and cyclone, respectively. All fields are composed of the 1982/83, 1991/92, and 1997/98 episodes.

Wang and Zhang (2002)

Monsoon-ENSO interaction (2)

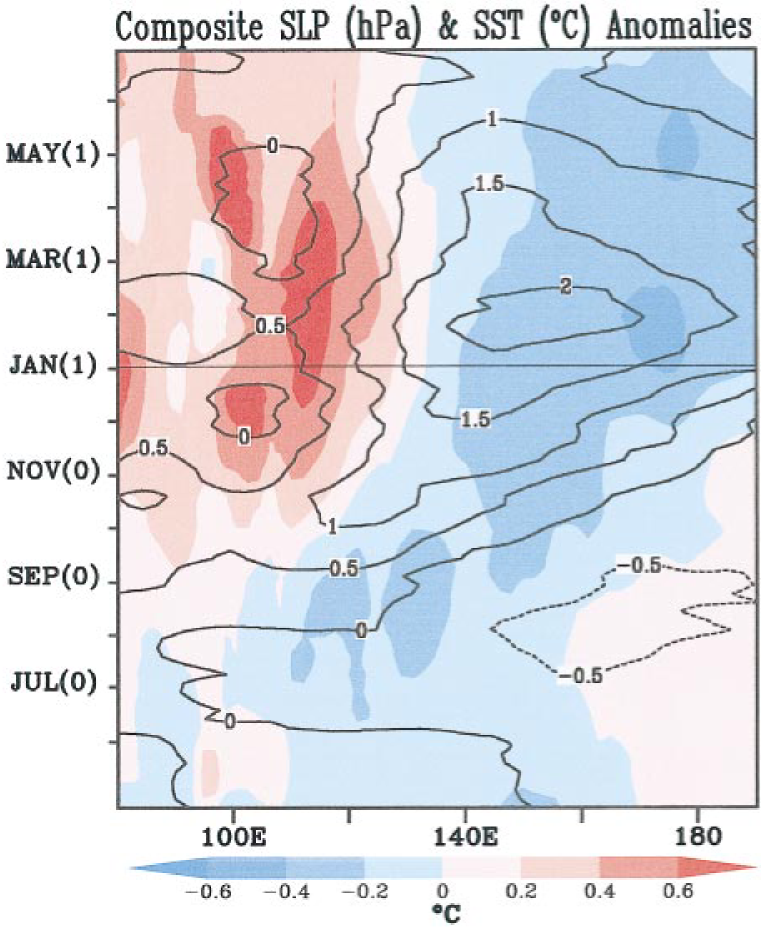

- PSAC straddling between cold and warm SST
- Note the eastward migration of whole system

Longitude–time diagram of the monthly mean sea level pressure (contours) and SST/land surface temperature (color shading) anomalies averaged for the latitude belt between 10 and 20N. The anomaly fields are composed of the six major El Nino events shown in Fig. 1. The time ordinate runs from May of year 0 to Jul of year 1, where the 0 and 1 denote the year during which ENSO warming develops and decays, respectively. The temperature between 100 and 110E is primarily the land surface temperature.

Monsoon-ENSO interaction (2)

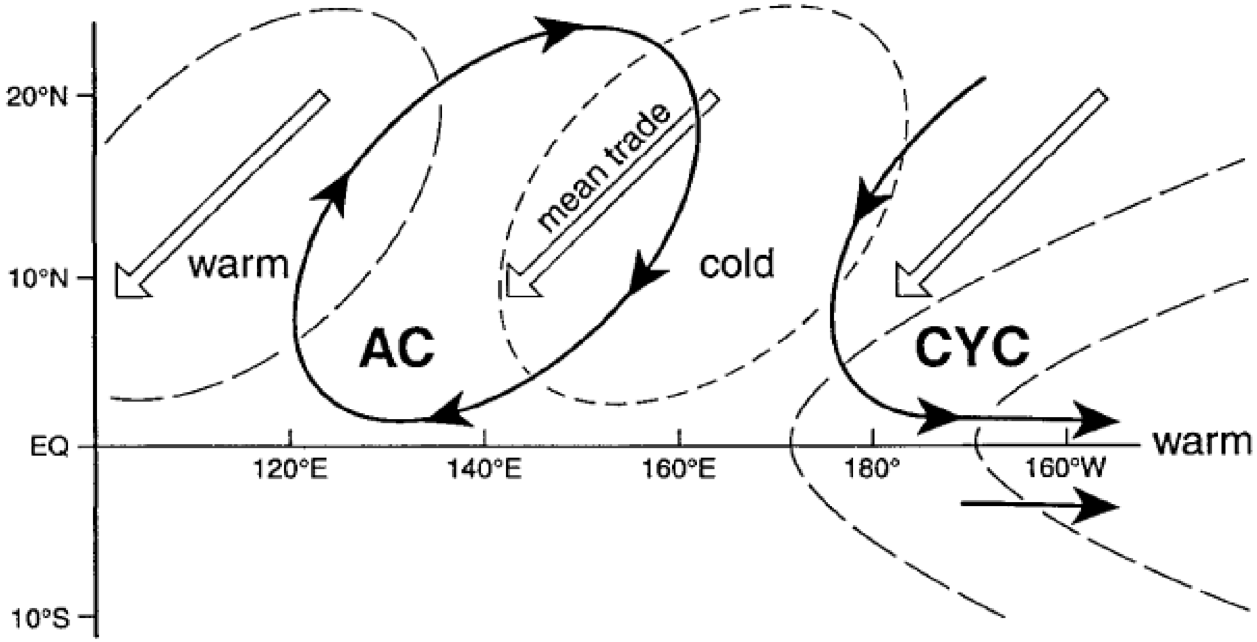

Wang et al. (2000)

Schematic diagram showing the air–sea interaction in the western North Pacific that maintains the Philippine Sea anticyclonic anomalies and associated negative SST anomalies in the western North Pacific. The double arrows denote the mean trade winds. The heavy lines with black arrows represent the anomalous winds. The long (short) dashed lines indicate contours of positive (negative) SST anomalies.

Monsoon-ENSO interaction (2)

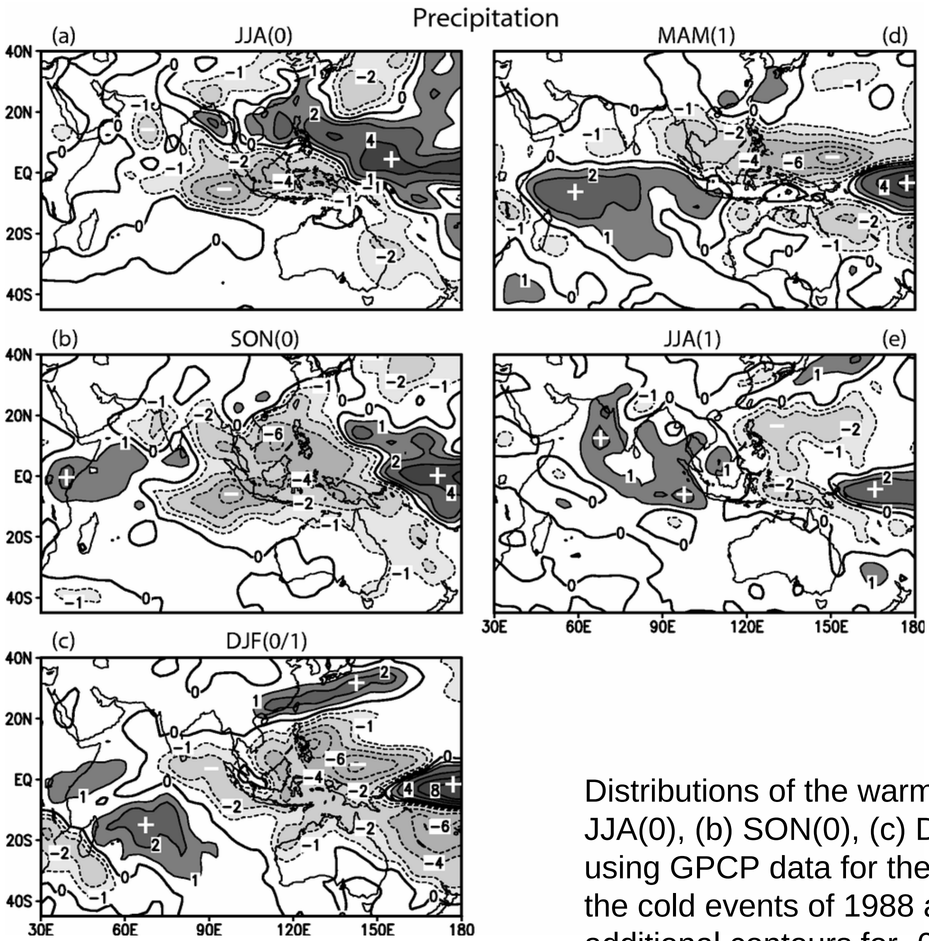

Distributions of the warm-minus-cold composites of precipitation during (a) JJA(0), (b) SON(0), (c) DJF(0/1), (d) MAM(1) and (e) JJA(1), as computed using GPCP data for the warm ENSO events of 1982, 1991 and 1997 and the cold events of 1988 and 1998. Contour interval: 1 mm d-1, with additional contours for -0.5 and +0.5 mm d-1 being inserted. Solid and dashed contours indicate positive and negative values, respectively.

Monsoon-ENSO interaction (2)

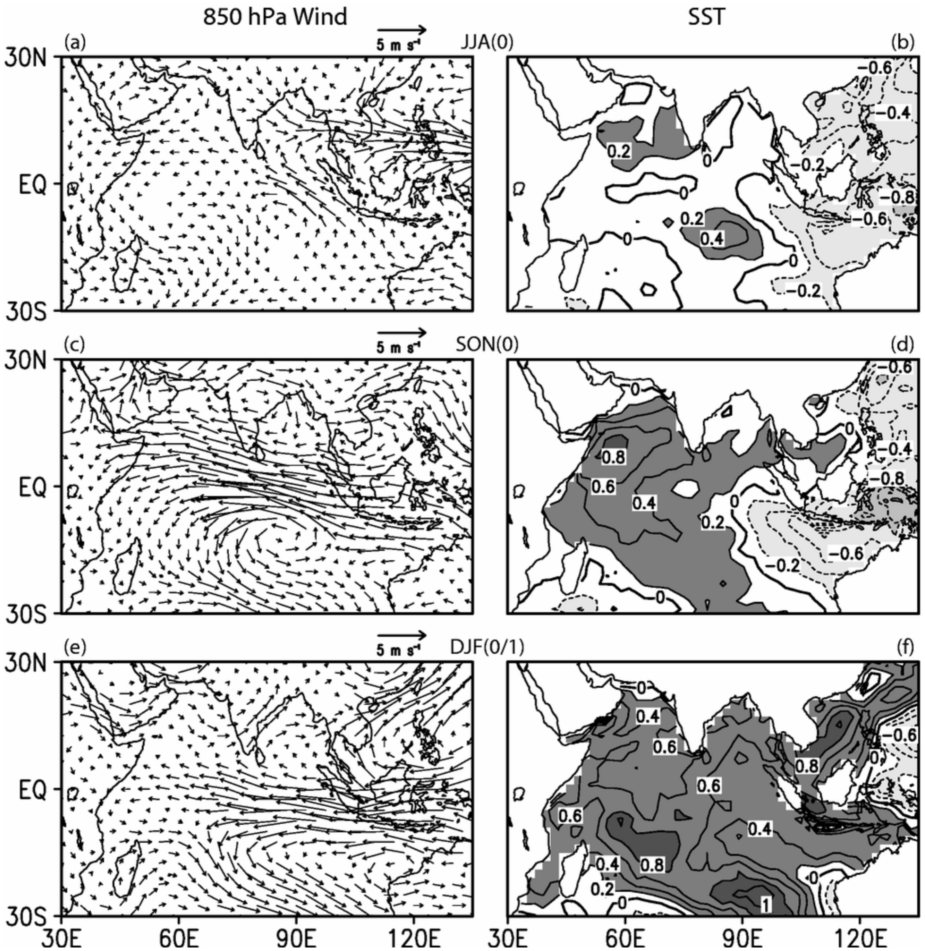

Distributions of the warm-minus-cold composites of 850 hPa vector wind (left panels) and SST (right panels; contour interval: 0.2oC) fields, for (a, b) JJA(0), (c, d) SON(0) and (e, f) DJF(0/1). Results are based on NCEP reanalysis data for six selected warm ENSO events and six cold events. Solid and dashed contours indicate positive and negative values, respectively.

Monsoon-ENSO interaction (2)

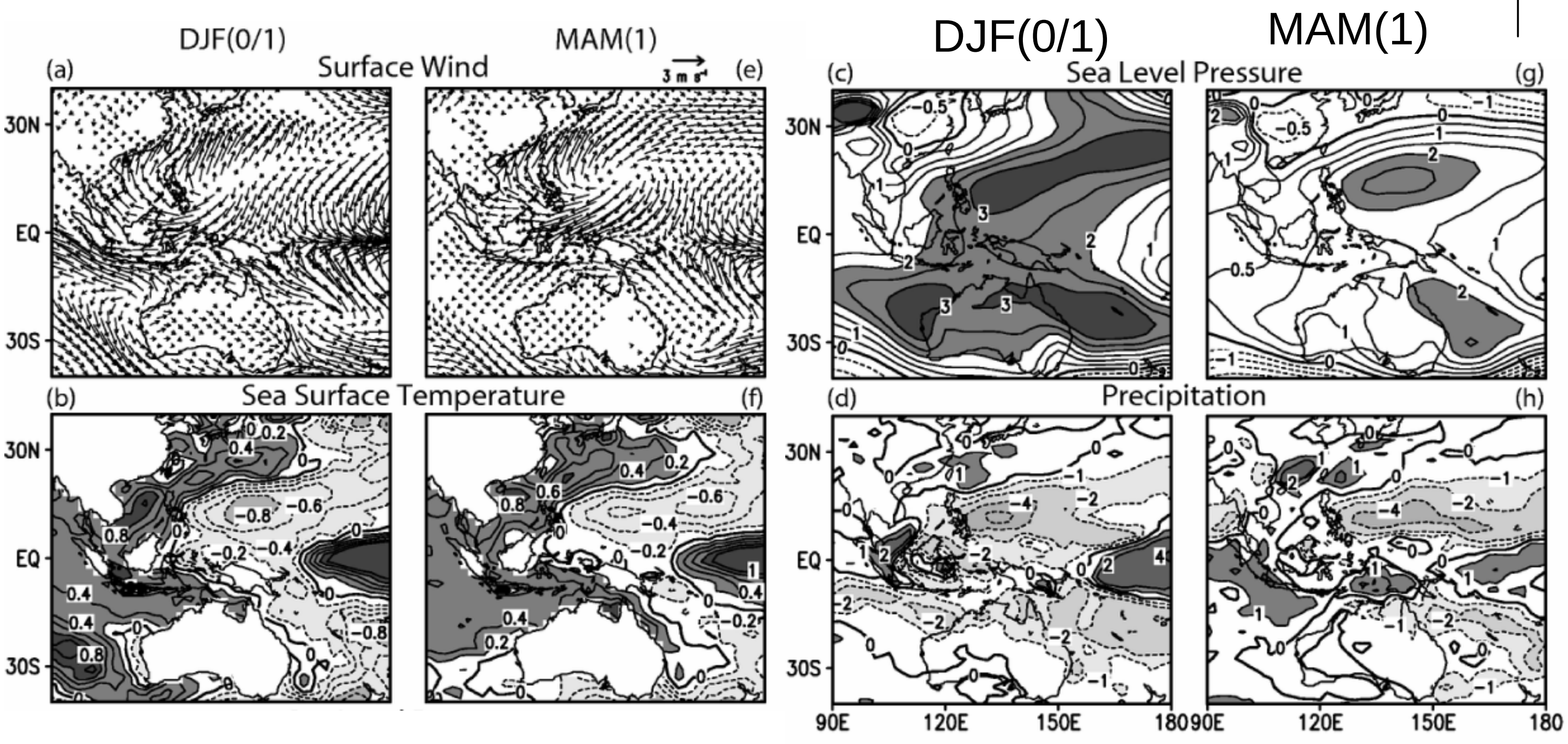

Distributions of the warm-minus cold composites of (a, e) surface wind vector, (b, f) SST (contour interval: 0.2˚C), (c, g) SLP (contour interval: 0.5 hPa), and (d, h) precipitation (contour interval: 1 mm d-1, with additional contours for -0.5 and +0.5 mm d-1 being inserted) for DJF(0/1) (left panels) and MAM(1) (right panels). Results are based on NCEP reanalysis data for six selected warm ENSO events and six cold events. Solid and dashed contours indicate positive and negative values, respectively.

Simulation of monsoon variability

Simulating monsoon variability

Numerical experiment with interactive ocean (mixed layer model)

model

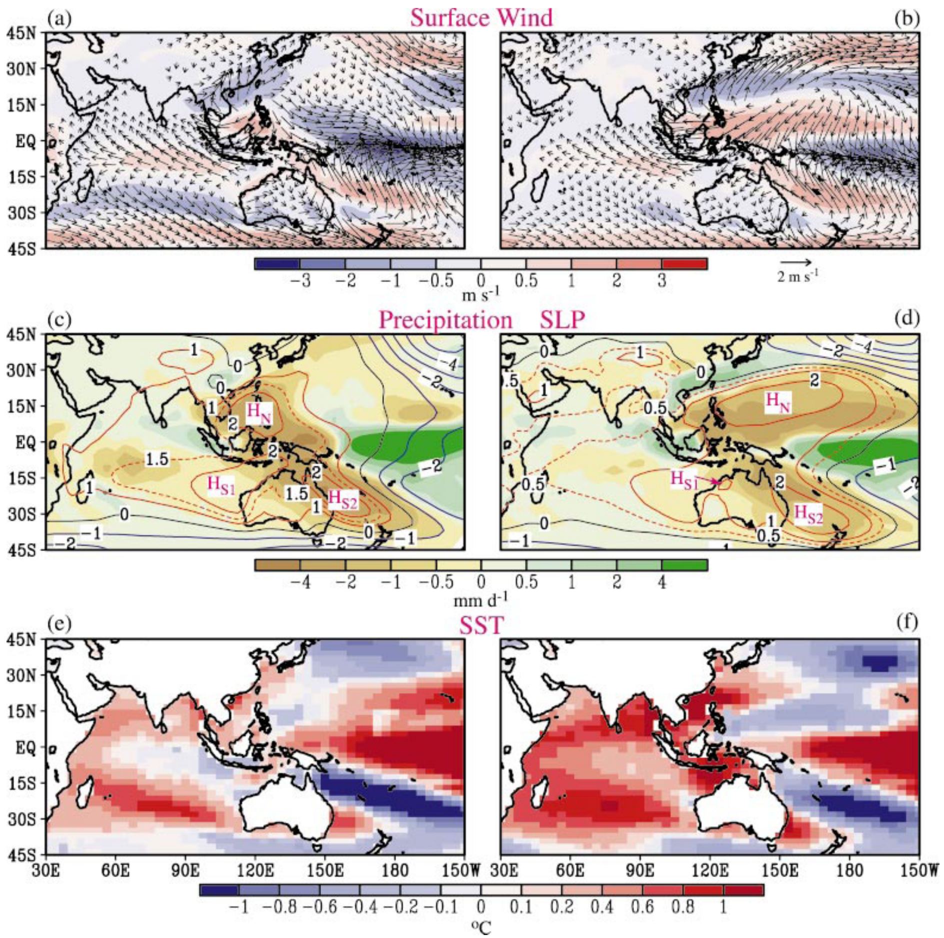

Obs

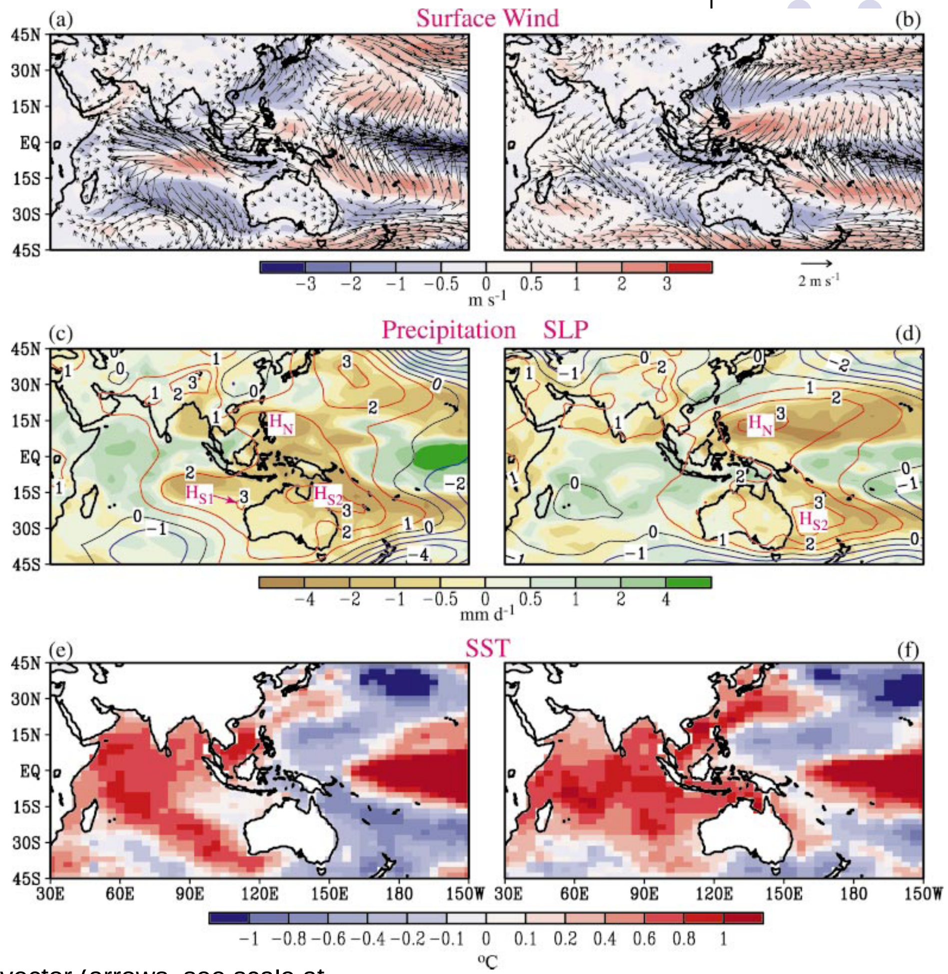

Distributions of the warm minus cold composites of the (a), (b) surface wind vector (arrows, see scale at bottom right) and surface wind speed (shading); (c), (d) precipitation (shading) and sea level pressure (contours, interval between solid isolines: 1 mb); and (e), (f) SST (shading). Results for the ONDJ(0/1) and FMAM(1) periods are presented in (a), (c), (e) and (b), (d), (f), respectively. All data are based on output from the MLM experiment. The labels HN, HS1, and HS2 in (c), (d) indicate the positions of the anomalous subtropical high pressure centers. In this and following figures, the color scale used for defining the shading in a given panel is shown below that panel.

Simulating monsoon variability

Interactive minus Non-interactive ocean

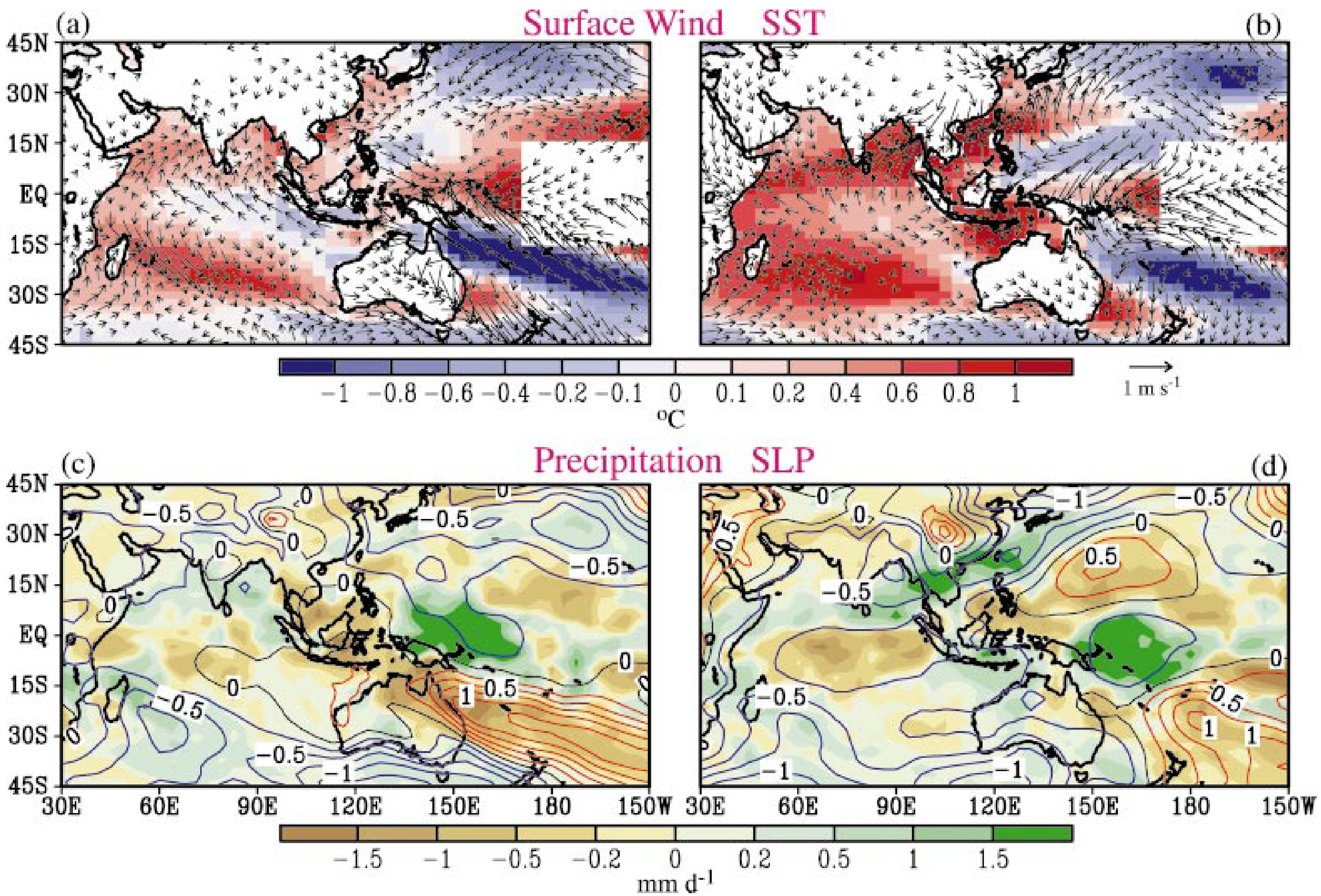

Distributions of the differences between the MLM and CTRL experiments, as obtained by subtracting the warm minus cold composites based on CTRL output from those based on MLM data, for (a), (b) surface wind vector (arrows, see scale at bottom right) and SST (shading); and (c), (d) precipitation (shading) and sea level pressure (contours, interval: 0.25 mb). Results for the ONDJ(0/1) and FMAM(1) periods are presented in (a), (c) and (b), (d), respectively.

Monsoon predictability-on-going research

(Soo-Jin Sohn, Daisuke Nohara, Bong-Geun Song, F.Tam, Saji H.)

East Asian Winter Monsoon

- There have been many efforts to understand the winter climate, and to predict the variation of the winter monsoon circulation in East Asia (Zhang et al., 1997, Jhun et al., 2004)

- The wintertime circulation of the East Asian continent is characterized by strong Siberian high and active cold surges, which strongly affect the local weather in the region (Hui, 2007).

- Most modeling studies for east Asian monsoon focused on summer time.

Models and Data

- **Models**

Acronym	Participating Institute	I.C. (Ens)	B.C (SST)
CWB	Central Weather Bureau (Chinese Taipei)	5	OSST
GCPS	Seoul National University (Korea)	12	FSST
GDAPS_F GDAPS_O	Korea Meteorological Administration (Korea)	20	FSST PSST
HMC	Hydrometerological Centre of Russia (Russia)	20	PSST
IRI	International Research Institute for Climate Prediction (USA)	24	OSST
JMA	Japan Meteorological Agency (Japan)	5	PSST / FSST
NCEP	NCEP Coupled Forecast System (USA)	15	CGCM

- **Data**
  - Hindcast Period : Winter form 1983/4 to 2003/4 (Dec.-Jan.-Feb. Monthly)
  - Variables : SLP, T850, UV850
  - Observed data :NCEP/NCAR Reanalysis

Winter Time Characteristics

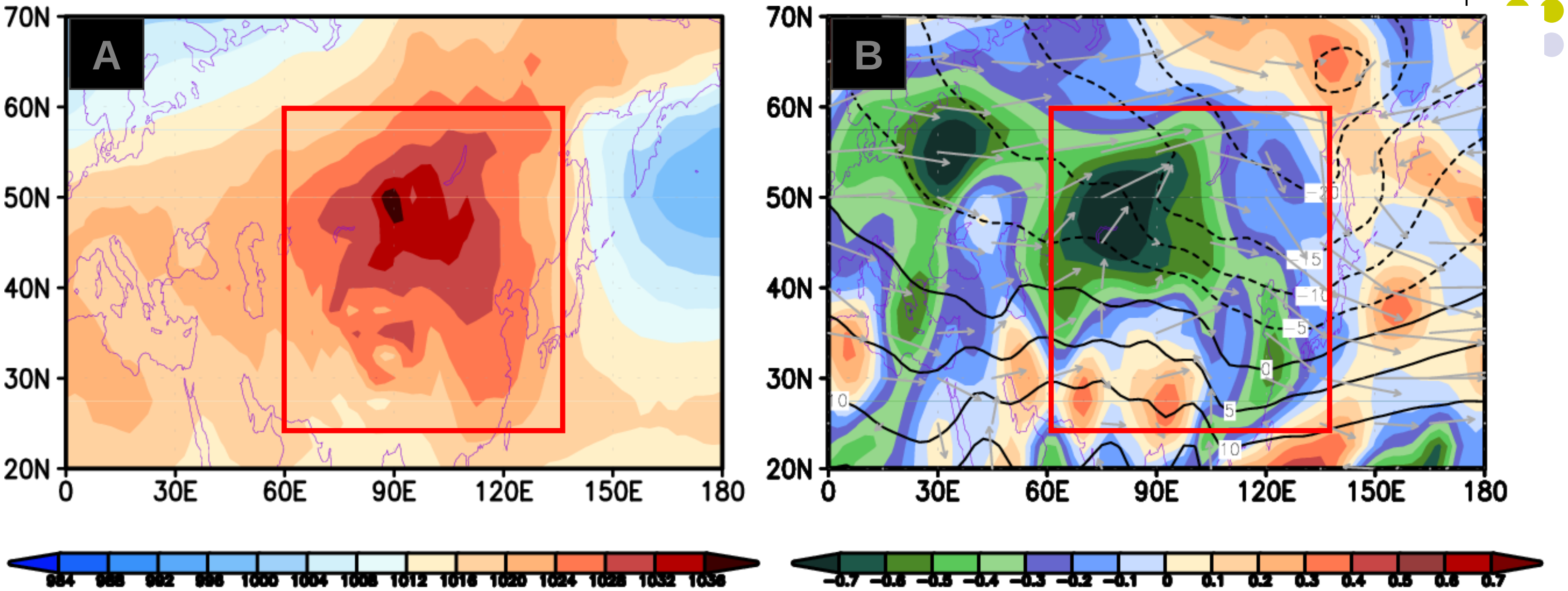

A. Climatology of SLP

B. Skewness of T850 (Shaded), Climatology of T850 (Contour),

Climatology of Wind at 850hPa(Vector)

☐ Interest Region (Box for EOF analysis)

Climatological Mean SLP for DJF

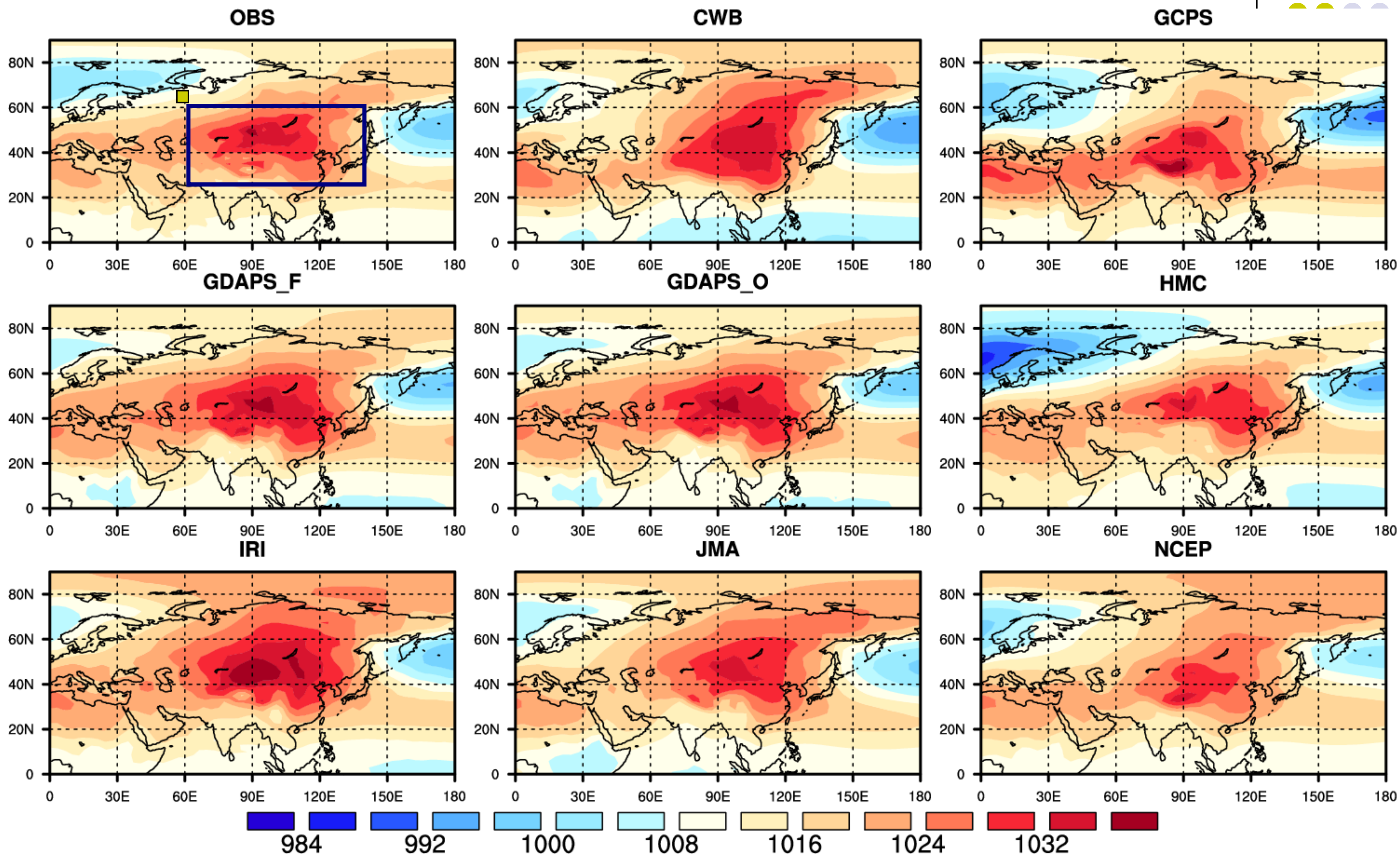

Skewness of T850 & Mean field of 850, temp & wind

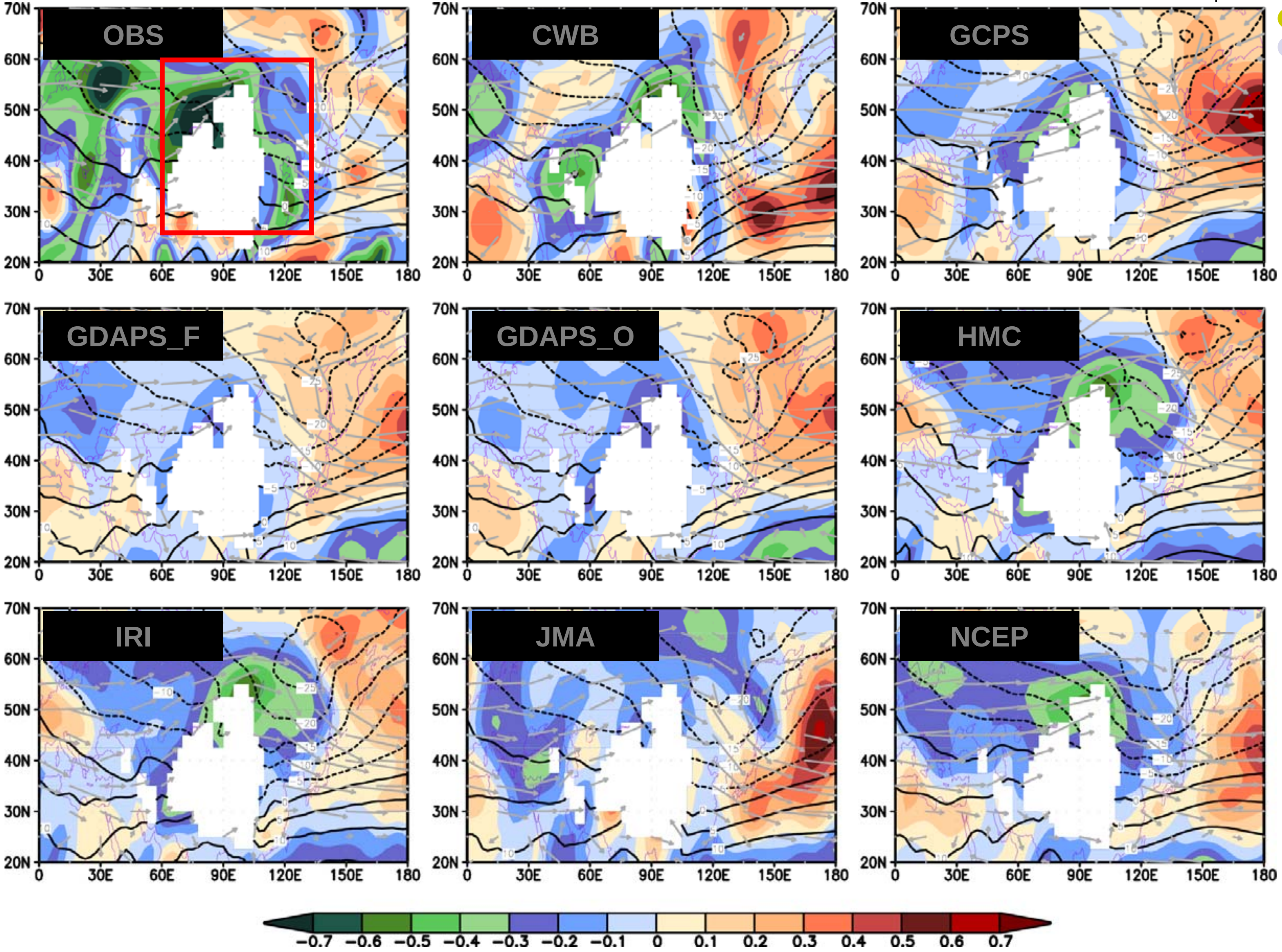

Results of Multivariate EOF (using T,V-wind)

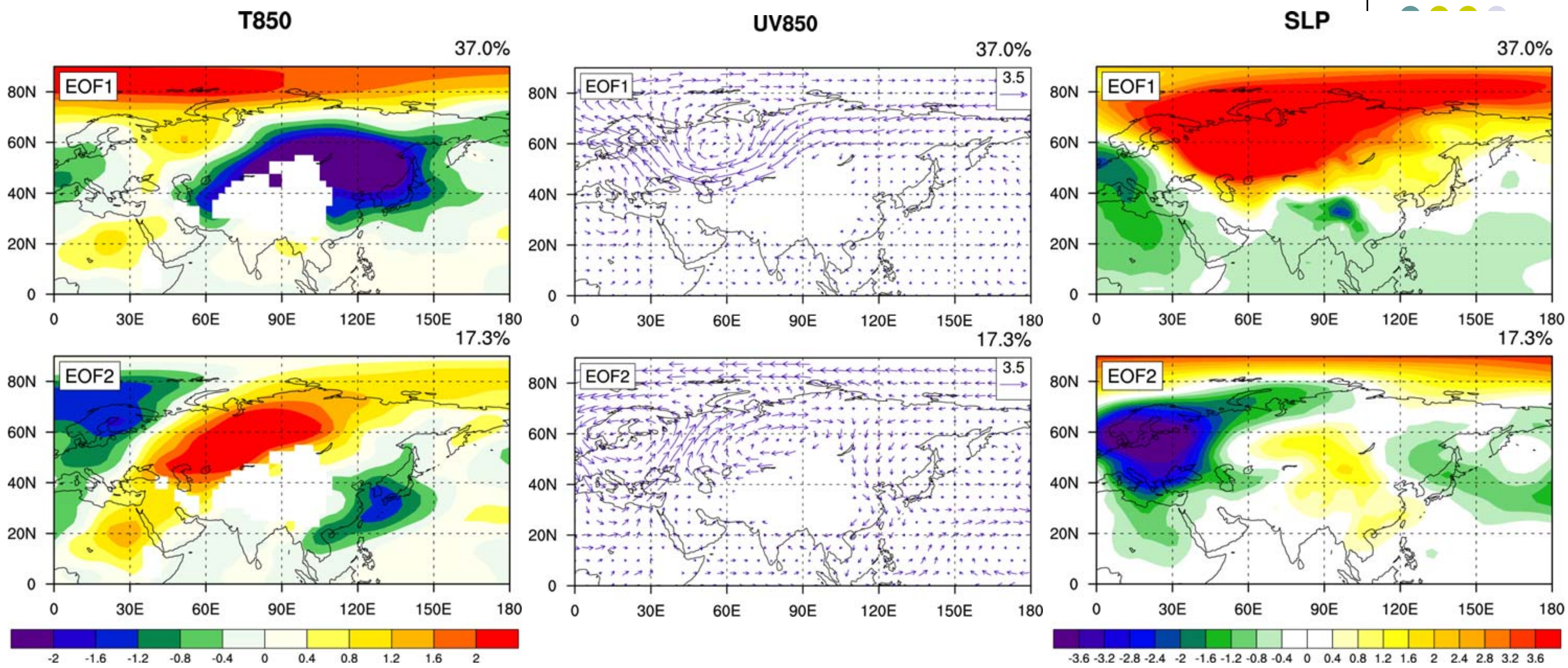

Correlation w/ major modes of climate variability:

CORR	PC1	PC2
AO	-0.37	-0.20
EU	0.25	0.60
Nino3.4	-0.10	0.04

Composites of Multivariate EOF 2

Anomaly Composite based on PC 2 (Cold Event)

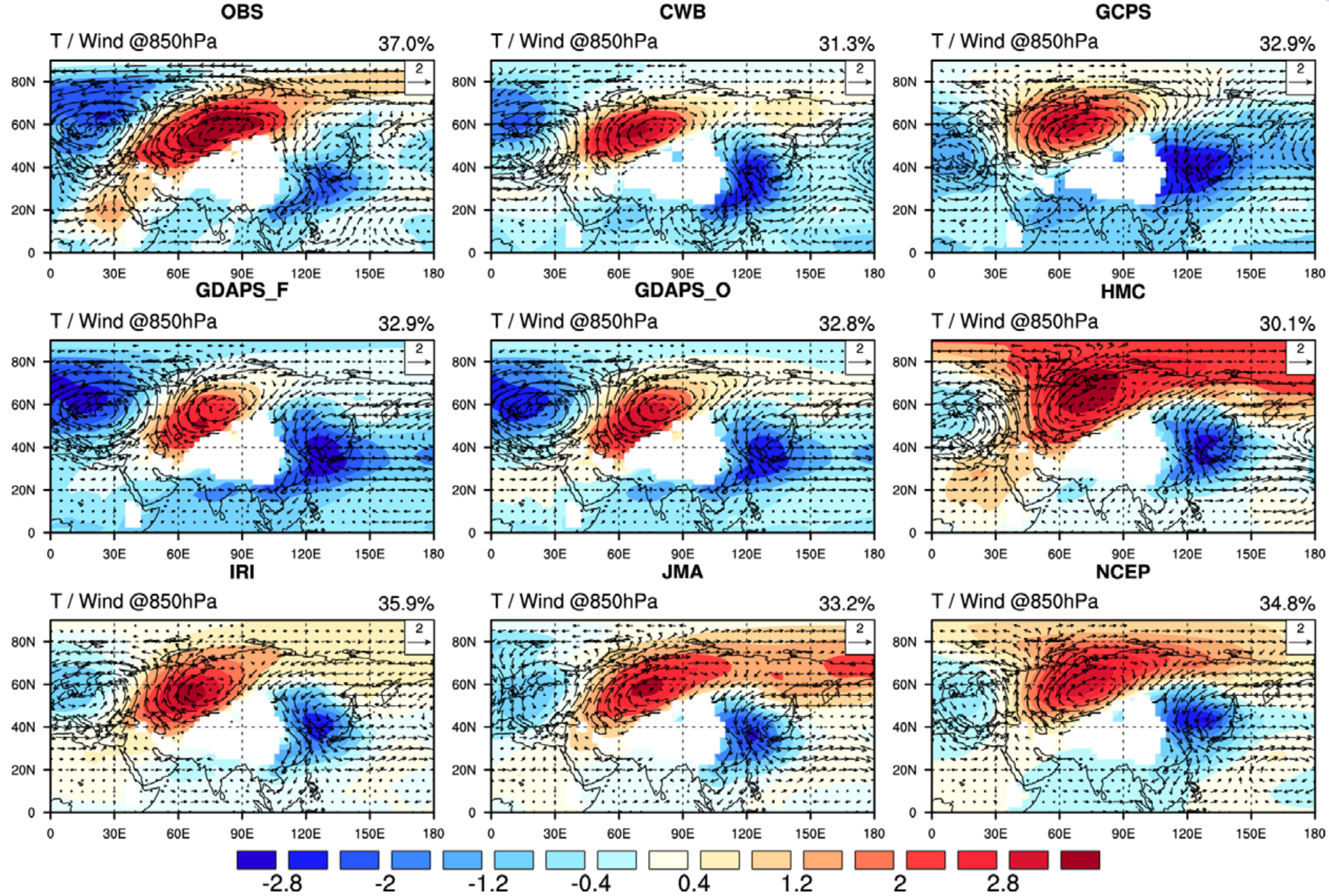

Predictability

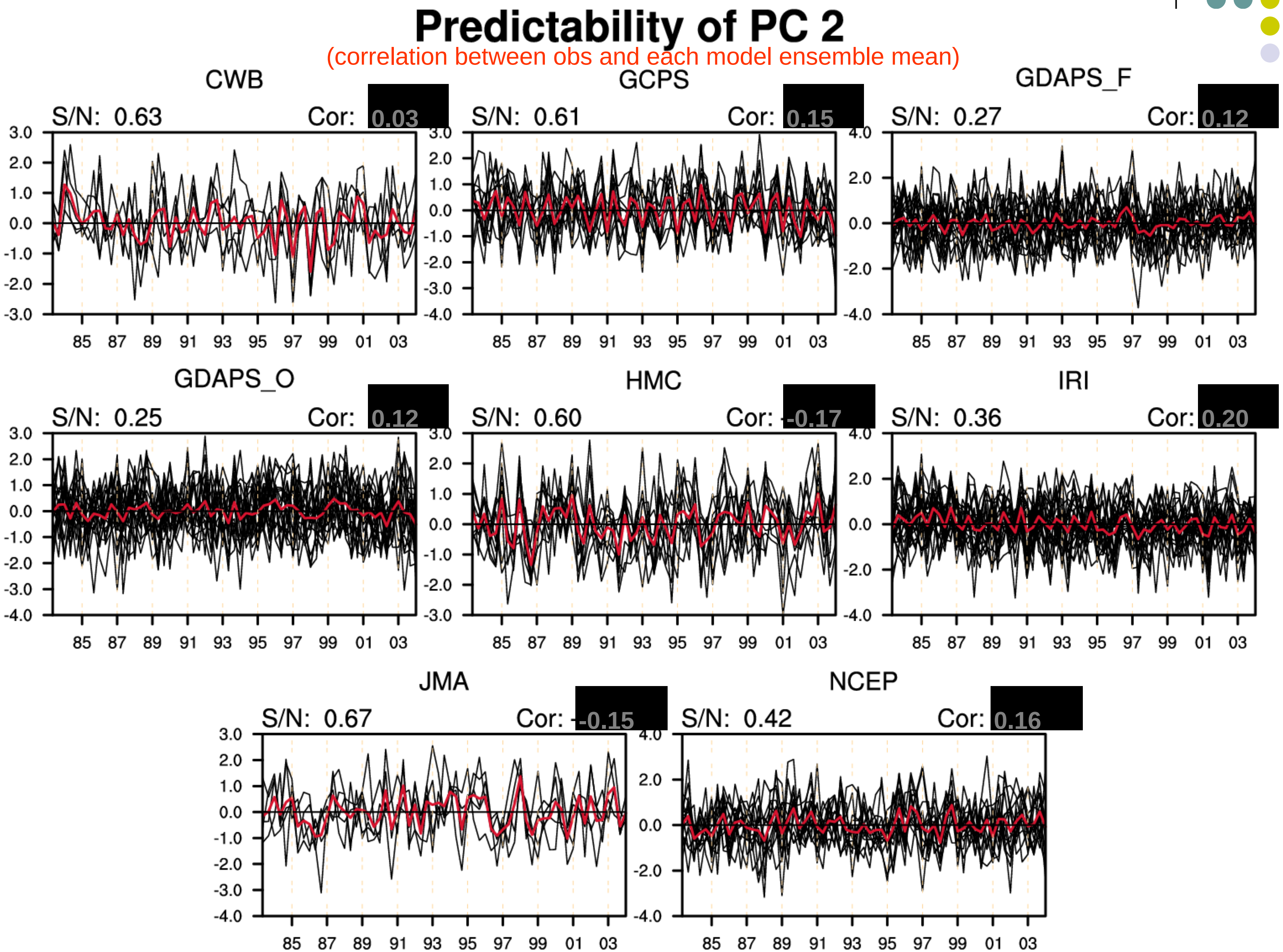

Connection w/ upper-level wavetrain

Z500

OBS

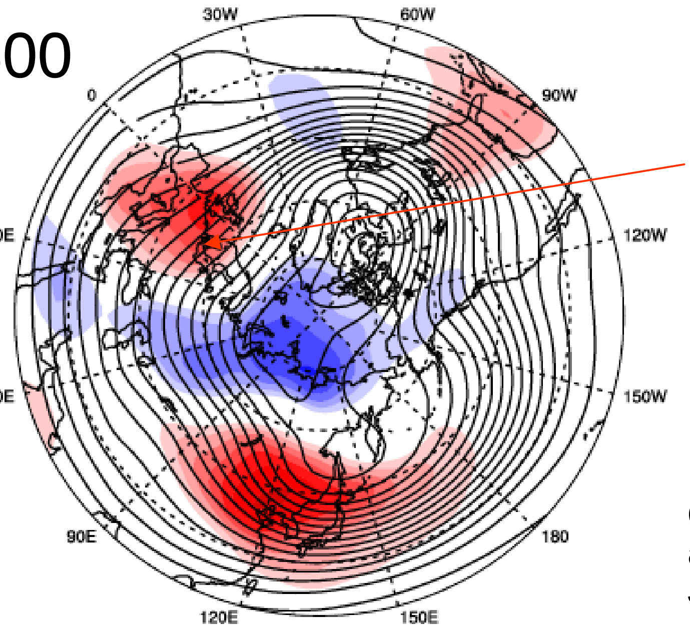

Models have difficulty simulating this link

Correlation coefficient between each grid of each variables and area averaged temperature at T850 over East Asia in January.

T850

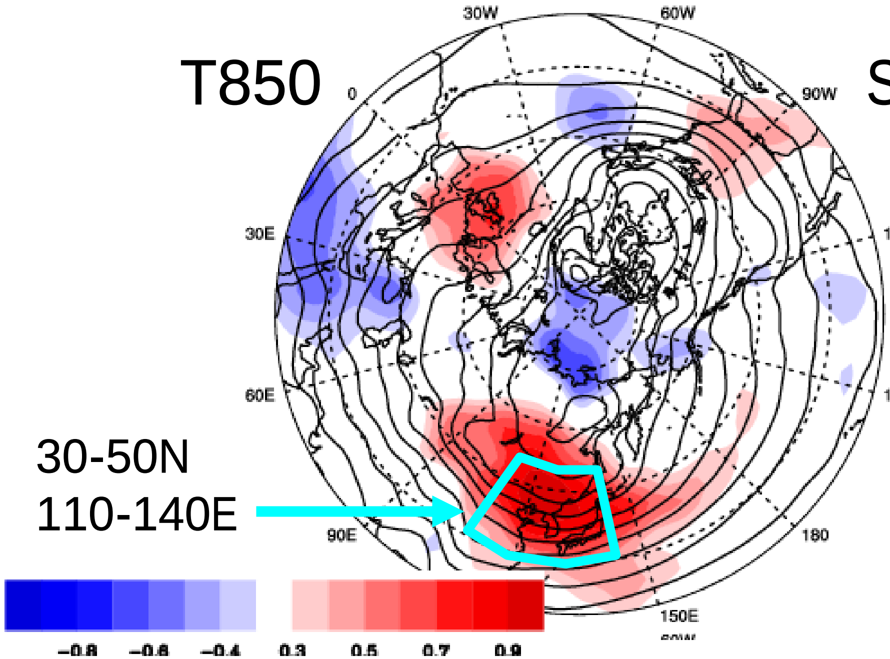

30-50N
110-140E

SLP

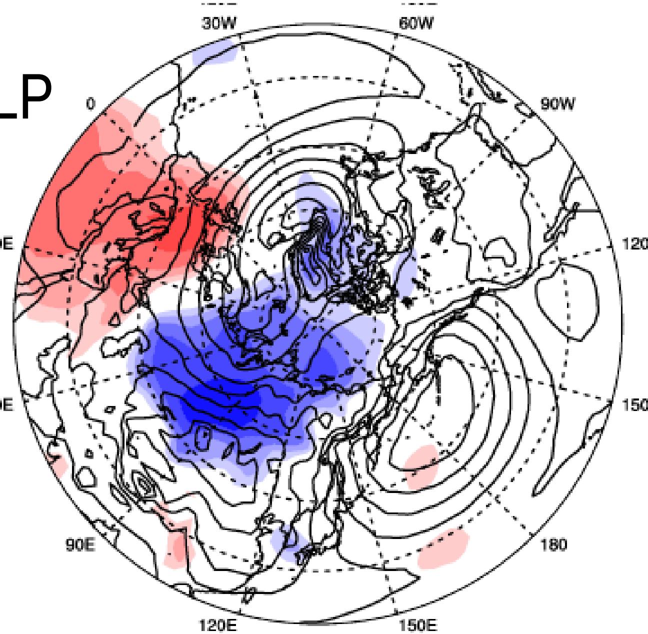

East Asian Summer Monsoon

Multivariate EOF 1st-mode of Wind at 850hPa (1983-2003): JJA Mean

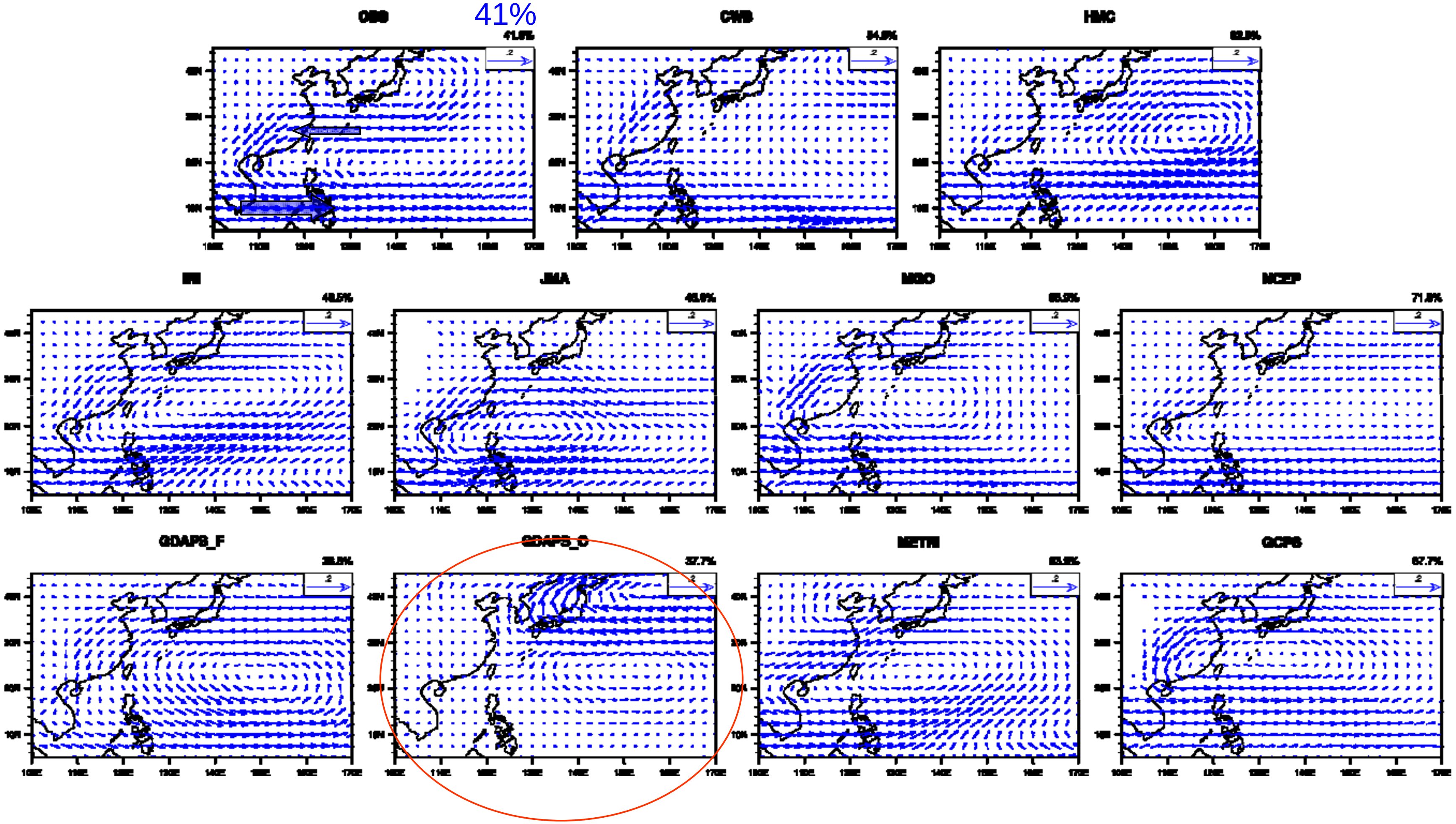

East Asian Summer Monsoon

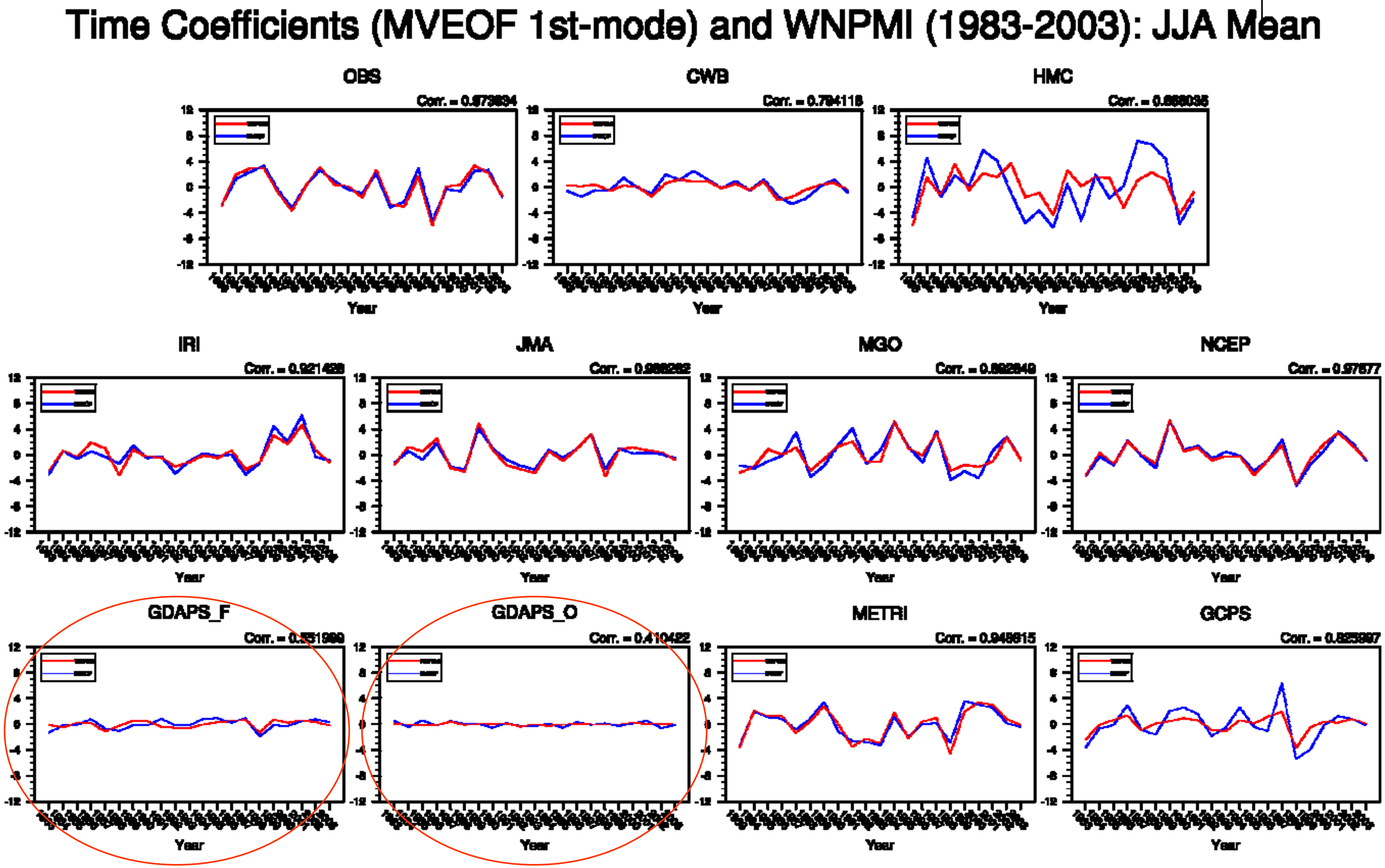

East Asian Summer Monsoon

Correlation Maps Between WNPMI and Precipitation (1983-2003): JJA Mean

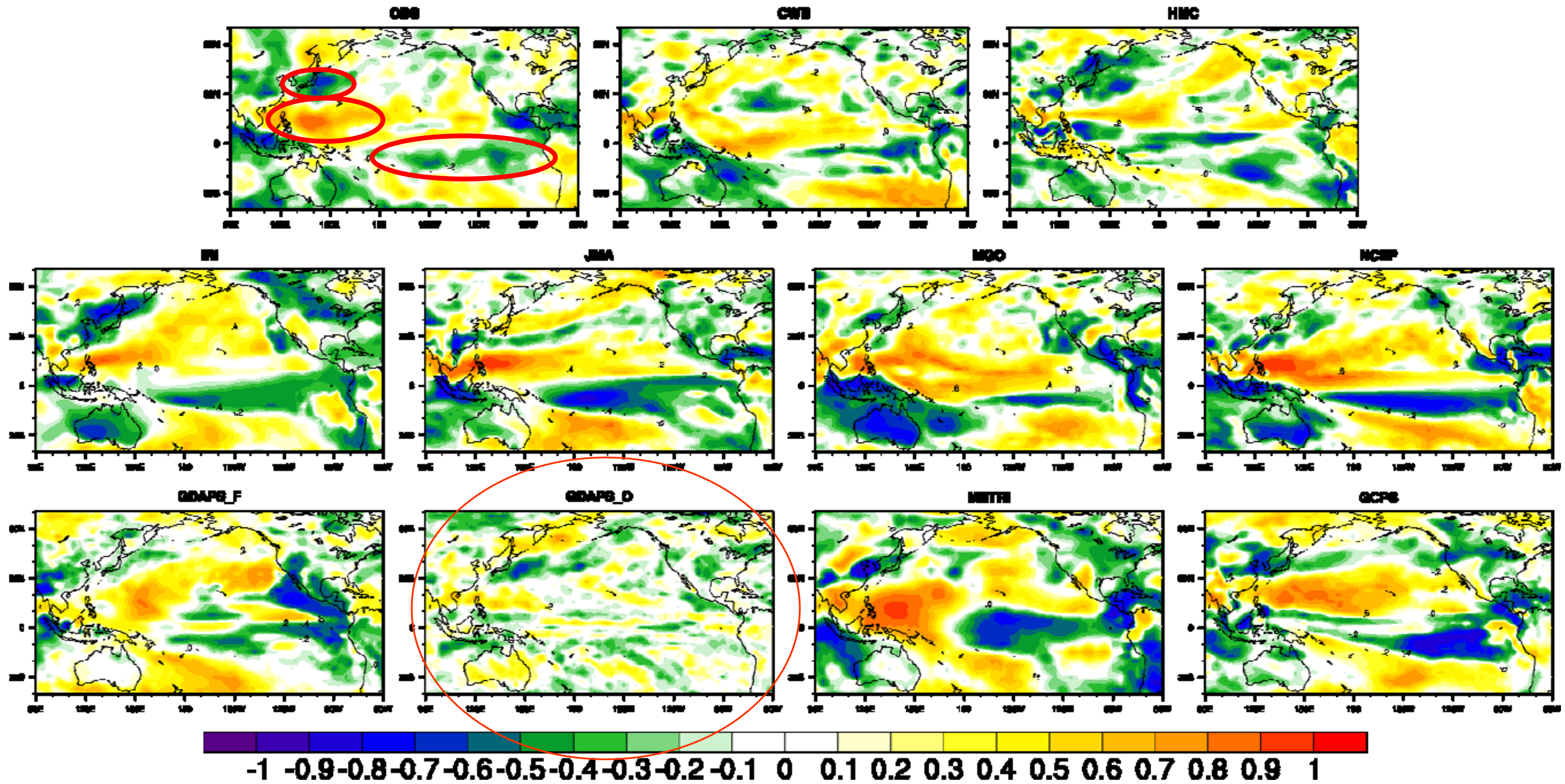

East Asian Summer Monsoon

Strong WNPMI minus Weak WNPMI (1983-2003): JJA Mean Wind850

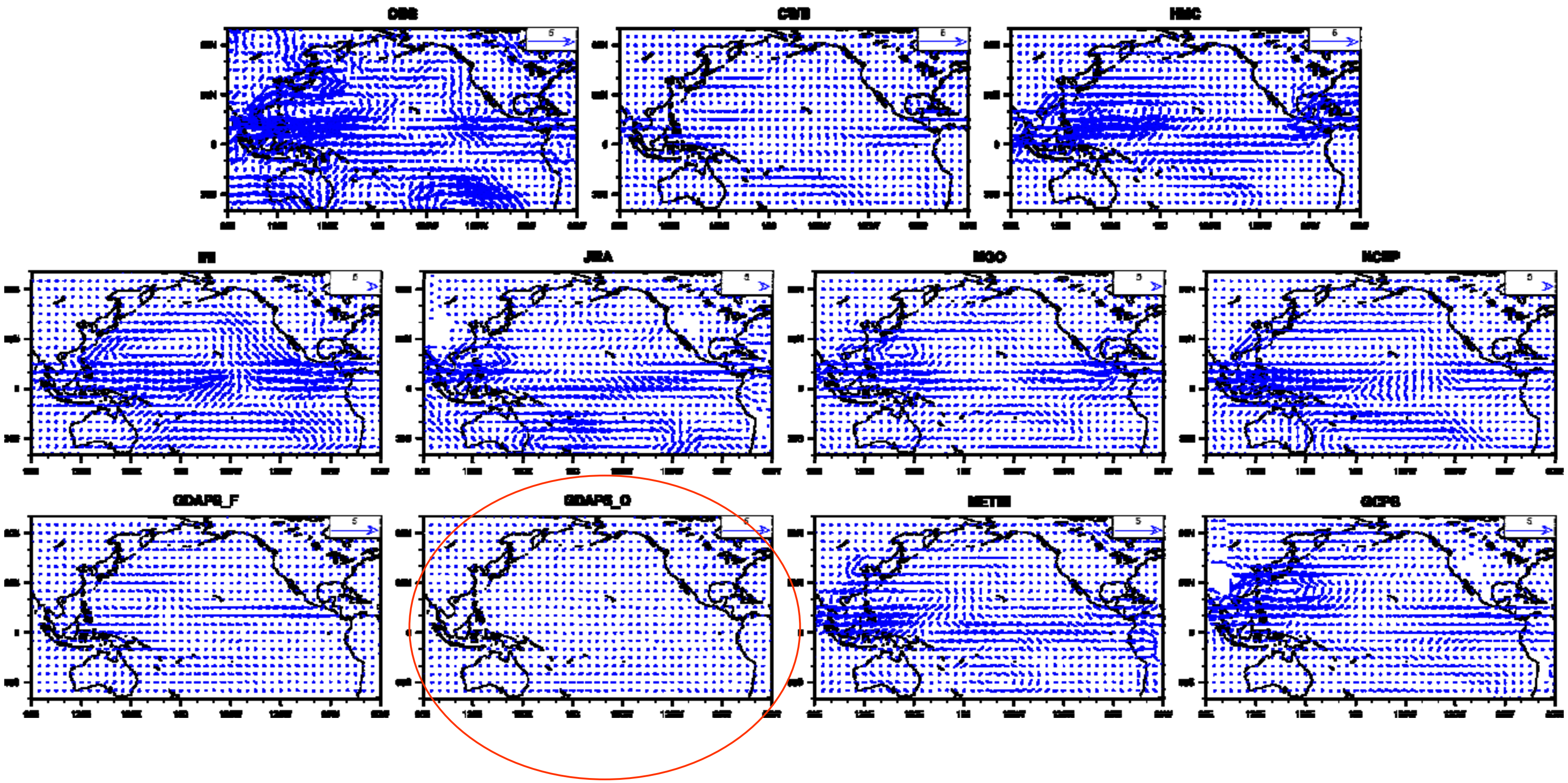

East Asian Summer Monsoon

Model Predictability - WNPSM

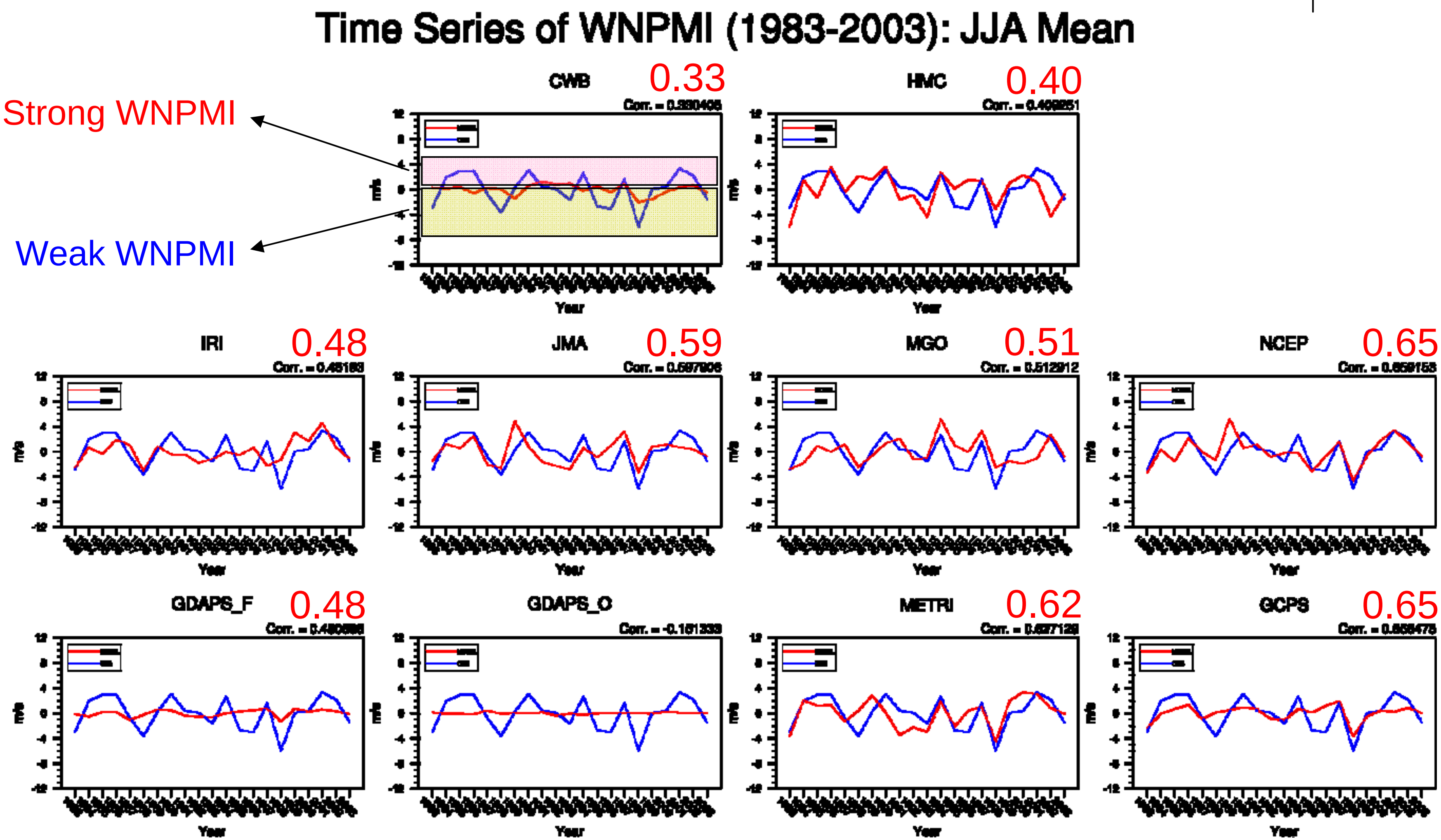

Correlation between model and obs for WNPMI

East Asian Summer Monsoon

- How to select models to form the best MME?
- Why does the MME work so well?

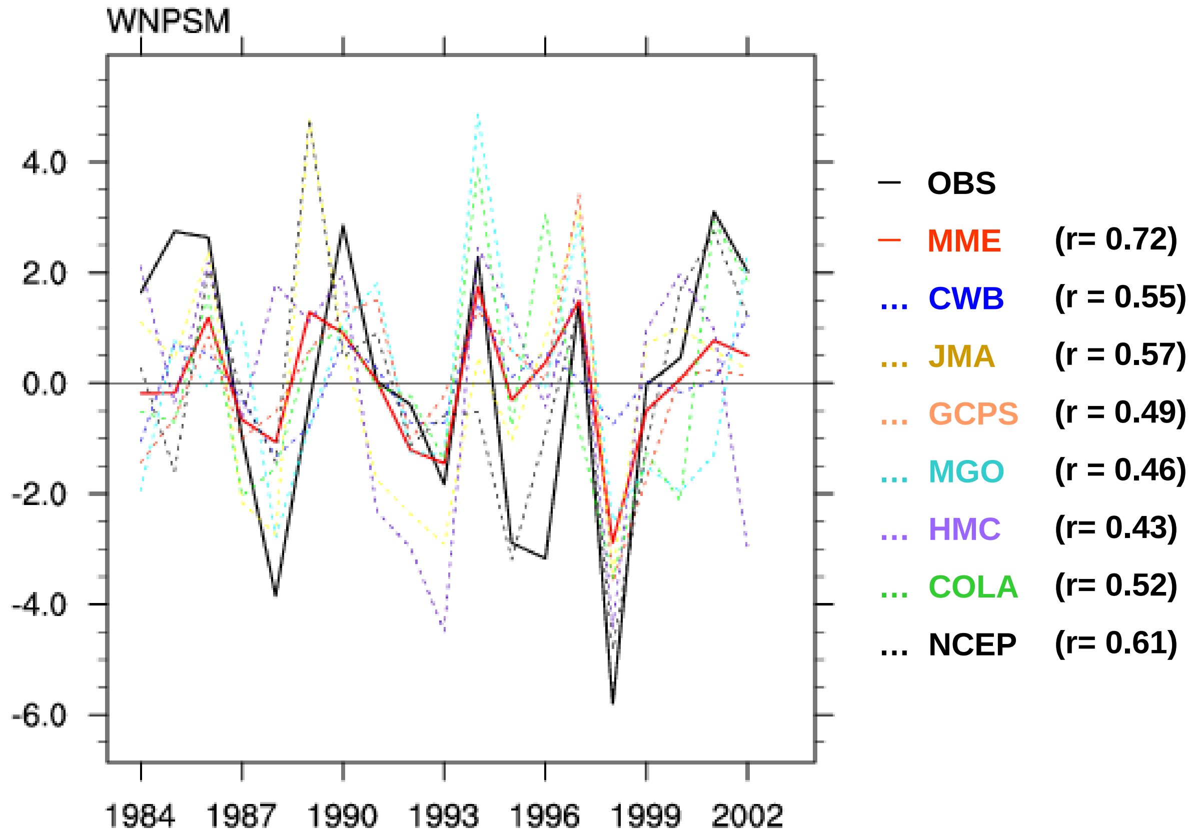

Other Topics: MJO prediction

MJO monitoring and prediction

- CPC/NOAA
  http://www.cpc.noaa.gov/products/precip/CWlink/MJO/mjo.shtml#current
- BoM Australia
  http://www.bom.gov.au/bmrc/clfor/cfstaff/matw/maproom/RMM/